

**ornl**

ORNL  
MASTER COPY

NOV 19 1982

ORNL/TM-12191

**OAK RIDGE  
NATIONAL  
LABORATORY**

**MARTIN MARIETTA**

Supplement to a  
Hydrologic Framework for  
the Oak Ridge Reservation,  
Oak Ridge, Tennessee

G. K. Moore  
L. E. Toran

Environmental Sciences Division  
Publication No. 3982



MANAGED BY  
MARTIN MARIETTA ENERGY SYSTEMS, INC.  
FOR THE UNITED STATES  
DEPARTMENT OF ENERGY

This report has been reproduced directly from the best available copy.

Available to DOE and DOE contractors from the Office of Scientific and Technical Information, P.O. Box 62, Oak Ridge, TN 37831; prices available from (615) 576-8401, FTS 626-8401.

Available to the public from the National Technical Information Service, U.S. Department of Commerce, 5285 Port Royal Rd., Springfield, VA 22161.

This report was prepared as an account of work sponsored by an agency of the United States Government. Neither the United States Government nor any agency thereof, nor any of their employees, makes any warranty, express or implied, or assumes any legal liability or responsibility for the accuracy, completeness, or usefulness of any information, apparatus, product, or process disclosed, or represents that its use would not infringe privately owned rights. Reference herein to any specific commercial product, process, or service by trade name, trademark, manufacturer, or otherwise, does not necessarily constitute or imply its endorsement, recommendation, or favoring by the United States Government or any agency thereof. The views and opinions of authors expressed herein do not necessarily state or reflect those of the United States Government or any agency thereof.

ORNL/TM-12191

**SUPPLEMENT TO A HYDROLOGIC FRAMEWORK  
FOR THE OAK RIDGE RESERVATION**

By G. K. MOORE

**SUMMARY OF GROUNDWATER MODELING**

By L. E. Toran

Date Issued--November 1992

Prepared by  
Environmental Sciences Division  
Oak Ridge National Laboratory  
ESD Publication 3982

Prepared for  
U.S. Department of Energy  
Office of Environmental Restoration and Waste Management  
under budget and reporting code EW 20

OAK RIDGE NATIONAL LABORATORY  
Oak Ridge, Tennessee 37831-6285  
managed by  
MARTIN MARIETTA ENERGY SYSTEMS, INC.  
for the  
U.S. DEPARTMENT OF ENERGY  
under contract DE-AC05-84OR21400

**Author Affiliation**

G. K. Moore is a research associate with the Civil Engineering Department at The University of Tennessee, Knoxville. L. E. Toran is a research associate with Martin Marietta Energy Systems, Inc., Earth and Atmospheric Sciences Section, Environmental Sciences Division, at the Oak Ridge National Laboratory.

TABLE OF CONTENTS

LIST OF FIGURES. . . . . v

LIST OF TABLES . . . . . vii

EXECUTIVE SUMMARY . . . . . ix

1. INTRODUCTION. . . . . 1

    1.1 Physiographic Setting . . . . . 3

    1.2 Geologic Setting. . . . . 5

    1.3 Hydrologic Setting. . . . . 6

2. OVERVIEW OF THE CONCEPTUAL MODEL. . . . . 8

3. PHYSICAL CHARACTERISTICS OF THE GROUNDWATER ZONE. . . . . 14

    3.1 Primary Porosity and Permeability . . . . . 14

    3.2 Porosity of Regolith, Saprolite, and Fractures. . . . . 15

    3.3 Occurrence and Significance of Pervious Fractures . . . . . 17

    3.4 Fracture Permeability . . . . . 25

    3.5 Relationship of Fractures and a Continuum . . . . . 30

    3.6 Groundwater Flow Paths. . . . . 33

4. SUMMARY OF HYDROGEOLOGIC CHARACTERISTICS. . . . . 36

5. CHEMICAL CHARACTERISTICS OF GROUNDWATER . . . . . 40

    5.1 Spatial and Temporal Variability of Water Chemistry  
        in Shallow Wells. . . . . 42

    5.2 Evidence for Grout Contamination. . . . . 46

    5.3 Evidence for Contaminant Flushing by Natural Processes 48

6. SUMMARY OF GROUNDWATER MODELING . . . . . 58

7. CONCLUSIONS . . . . . 67

8. REFERENCES. . . . . 71

APPENDIX: PROCEDURES USED TO OBTAIN DATA THAT ARE DESCRIBED  
OR INTERPRETED IN THE TEXT. . . . . A-1

    A.1 Procedures for Injection Tests. . . . . A-3

    A.2 Procedures for Hydrograph Analysis. . . . . A-5

    A.3 Procedures for Borehole Flowmeter Surveys . . . . . A-9

    A.4 References. . . . . A-12

•

•

•

•

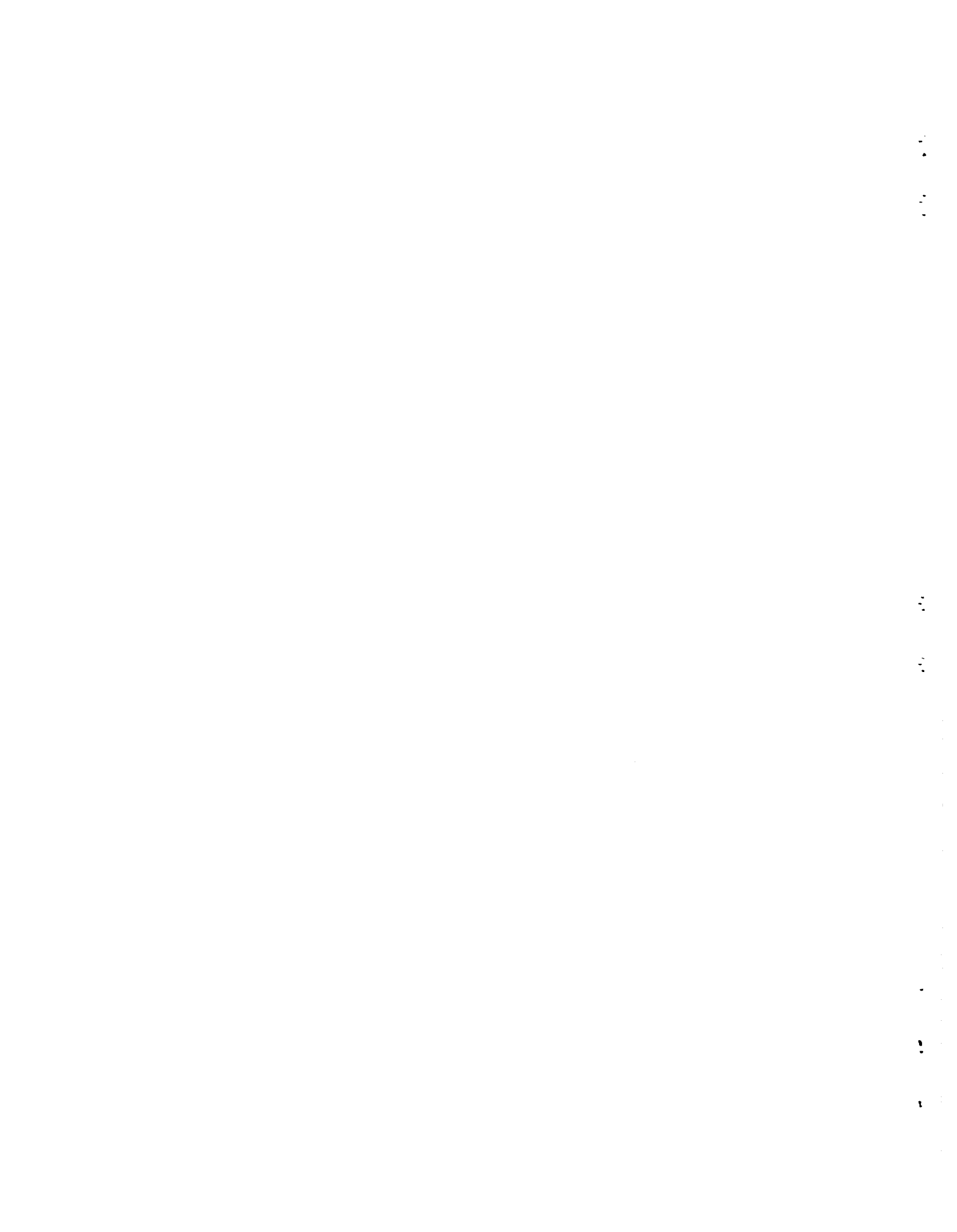
•

•

•

## LIST OF FIGURES

1	Location of the Oak Ridge Reservation and the three DOE facilities. . . . .	2
2	Locations of the Knox aquifer on the ORR. . . . .	9
3	Hydrogeologic zones and directions of water flow on the ORR . . . . .	12
4	Cumulative probability graph of fracture apertures calculated from transmissivity data . . . . .	16
5	Diagram showing relationship of pervious fractures to pervious sections and permeable intervals in a well . . .	18
6	Diagram showing geometry for the calculation of orthogonal fracture spacing . . . . .	20
7	Cumulative probability graphs for transmissivity data, which are calculated from slug tests and injection tests on the same wells . . . . .	26
8	Cumulative probability graph of hydraulic conductivity data for pervious fractures; data from injection tests and borehole flowmeter surveys. . . . .	27
9	Cumulative probability graphs of transmissivity values from early and late water level data during injection tests . . . . .	32
10	Location map and sections showing specific conductance of water ( $\mu\text{mhos/cm}$ ) and screened intervals in paired shallow and deeper wells near the junction of Whiteoak Creek and Melton Branch . . . . .	44
11	Relationship of the standard deviation of specific conductance to well depth . . . . .	46
12	Cumulative probability graph of nitrate concentrations, as nitrogen, in groundwater near the site of the S-3 Ponds, 1986-89. . . . .	50
13	Average normalized concentrations of nitrate as nitrogen in wells GW-106, GW-127, and GW-276. . . . .	52
14	Graph of average normalized concentrations for the major constituents in Bear Creek. . . . .	56



## LIST OF TABLES

1	Summary of hydrogeologic properties (average value or range) . . . . .	38
2	Temporal changes in the specific conductance of water for wells on hillslopes . . . . .	43
3	Temporal changes in the specific conductance of water for wells near streams. . . . .	43
4	Concentrations of major constituents in water from station 12.46 on Bear Creek during part of 1983. . . . .	53
5	Comparison of selected numerical models for groundwater flow on the Oak Ridge Reservation . . . . .	60
6	Index of numerical modeling codes . . . . .	66

1  
2  
3

4  
5  
6

7  
8  
9

## EXECUTIVE SUMMARY

The information in this report should prove useful for flow and contaminant-transport modeling of groundwater and for evaluating the alternatives for remedial action. New data on porosity and permeability have been analyzed and interpreted to produce a better understanding of the relationships between unfractured rock, low permeability intervals, and relatively permeable intervals. Specifically, the dimensions, orientations, depths, and spacings of pervious fractures have been measured or calculated; the depths and directions of subsurface flow paths (Solomon et al. 1992, pp. 3-21 to 3-23) have been corroborated with new data; fractures near the water table have been shown to have different characteristics than those at deeper levels; and the relationships between groundwater flows in fractures and flows in the continuum have been described. This is the information needed for the numerical modeling of groundwater flows.

Other information in this report should result in a better understanding of spatial and temporal differences in water chemistry, including changes in contaminant concentrations. Temporal changes in groundwater chemistry have been shown to occur mostly near the water table. These changes consist of a periodic dilution of chemical constituents by recharge and a slow increase in constituent concentrations between recharge events. At discharge locations, spatial differences in groundwater chemistry are integrated by mixing. The monitoring of water chemistry in streams near contaminant sources may produce a better indication of contaminant releases and trends than do the records obtained from a few upgradient and downgradient wells.

Water pollution on the Oak Ridge Reservation results from disposals and spills of radioactive, hazardous, and mixed wastes. With few exceptions, the problems are represented by (1) leachates from wastes and other contaminant sources, (2) secondary reservoirs of contaminants in the rock matrix along groundwater flow paths between disposal sites and surface streams, and (3) contaminated sediments in the streams. The transport of contaminated stream sediments is beyond the scope of this report, but erosion control is a common engineering problem that has alternative solutions. Contaminants in the rock matrix, within the area of a plume, can probably be ignored because the matrix is nearly impermeable, because release rates are slow and are determined by the rate of molecular diffusion, and because contaminant concentrations decrease through time as a result of groundwater recharge and discharge. The remaining problem, which is leaching of waste sources by subsurface flows of water, can be solved in most areas by hydrologic isolation.

Hydrologic isolation of contaminant sources requires either (1) grouting or vitrification of the wastes to produce a mass that is less permeable than the surrounding rocks, or (2) both capping to prevent water infiltration and a shallow, upgradient French drain to intercept and divert subsurface stormflow. The smaller the area that is capped, the more important is the diversion of stormflow. Nearly all of the wet-silo, bathtubting-trench, and ineffective-cap problems in the area of the Oak Ridge National Laboratory have been caused by lateral inflows of water in the stormflow zone. A combination of a surface cap and an upgradient drain should hydrologically isolate the contaminant sources that are above the water table. Within a 1-year period thereafter, the permeable layer below the water table should drain and cause an average 1-2 m drop in the water table; the seasonal fluctuations in the water table also should decrease.

## 1. INTRODUCTION

The Oak Ridge Reservation (ORR) (see Fig. 1) of the U.S. Department of Energy (DOE) lies between Oak Ridge, Tennessee and the Clinch River about 30 km west of Knoxville. The three DOE research and production facilities in this area of about 90 km<sup>2</sup> are the Oak Ridge Y-12 Plant, the Oak Ridge National Laboratory (ORNL), and the Oak Ridge K-25 site. Low-level radioactive waste and other wastes have been stored in shallow burial grounds near these facilities since 1943. The main problem resulting from the waste storage practices and from leaks and spills has been the mobility of contaminants in groundwater and surface water.

Presently, groundwater monitoring, site characterizations, and remedial actions are under way at the three DOE facilities as part of a comprehensive environmental restoration program. During 1989, the entire ORR was placed on the Environmental Protection Agency (EPA) National Priorities List. In response, a Federal Facilities Agreement was developed by DOE, EPA Region IV, and the Tennessee Department of Environment and Conservation. Implementation of the terms of this agreement and of DOE Order 5400.1 requires a comprehensive understanding of the hydrogeology of the ORR. Most of the remedial investigations at the DOE facilities are site specific and include only a single waste area grouping (WAG). Thus, the Oak Ridge Reservation Hydrology and Geology Study (ORRHAGS) was established in 1989 as an integrated study of hydrology, geology, and soils in support of all activities in environmental monitoring, environmental restoration, waste management, and regulatory compliance on the ORR. The hydrology phase of ORRHAGS is intended to develop a practical understanding of the relationships between wastes, hydrologic parameters and processes, flow paths, contaminant transport, and pollution of the surface and subsurface environment.

The first status report on the hydrology phase of the ORRHAGS project (Solomon et al. 1992) describes a conceptual model for the hydrogeology of the ORR as well as the implications of this model for the environmental restoration programs. The conceptual model is believed to represent the important hydrologic properties and processes on the ORR, but it is necessarily generalized and is not intended to describe the detailed characteristics of specific sites. Also, the model was developed from available data and is not completely detailed and definitive. On the other hand, the model explains the results of most previous studies and observations; it also provides a reliable description of water occurrence and flow, including most factors that affect contaminant fluxes and flow paths.

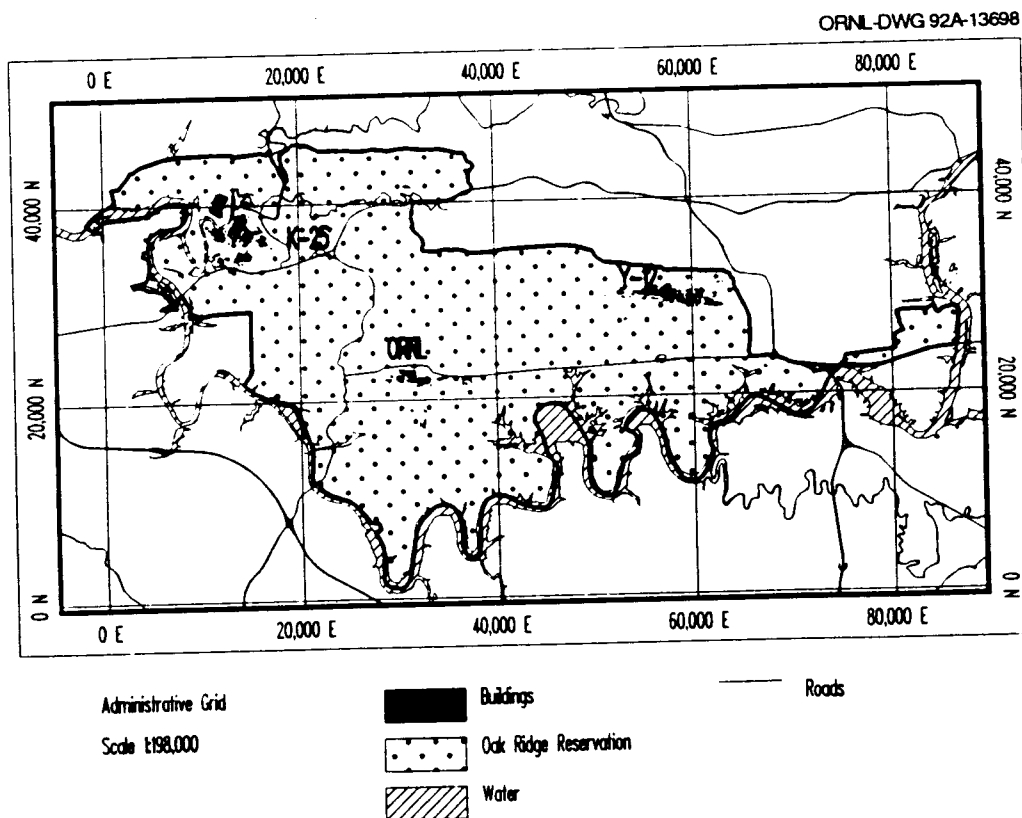


**Fig. 1. Location of the Oak Ridge Reservation and the three Department Of Energy facilities.**

This report has been prepared as a supplement to the conceptual model of the ORR (Solomon et al. 1992). Some data were unavailable when the status report was written and some new data have been acquired. This report neither changes the conceptual model nor describes the entire model in detail. Instead, several new aspects of the model and the significance of the new data are discussed. A brief description of the geology and hydrology of the area and a summary of the conceptual model are also included for background information.

Several terms in this report are different than those in other recent reports. Regardless of orientation, the dimensions of a single rock fracture are length, width, and aperture; groundwater flows along the length of a fracture, and the cross-sectional area for this flow is the product of width and aperture. Also, the thickness of a fracture or a permeable interval is a vertical measure in a well. Finally, a matrix interval has previously been defined as a fractured but relatively impermeable interval below the water table; here the term "matrix" is reserved for unfractured rock.

### 1.1 PHYSIOGRAPHIC SETTING

The ORR is located in the Valley and Ridge Province, which extends from New York to central Alabama. The elevations of the valleys on the ORR average about 235 m above mean sea level. The subparallel ridge crests trend northeast-southwest, are nearly accordant, and are about 90 m higher than the valleys. The topography has been formed by the erosion of folded sedimentary rocks that consist of alternating sequences of weakly resistant shales and shaley limestones and strongly resistant sandstones and dolostones. The southeast-facing sides of most ridges slope in the same direction as the rock layers; these back slopes are

longer than the northwest-facing front slopes. The southeast-facing back slopes also have an irregular topography, which is commonly hummocky to dissected, whereas the front slopes are steeper and smoother. Most cultural features, including the waste burial grounds, are located on the lower back slopes or in the adjacent valleys.

The Clinch River and the lower reaches of the larger tributaries flow through incised meanders, the wavelengths of which vary with stream size and the azimuth of the thalweg. Smaller streams are a pool-and-riffle type; the drainage patterns are a dendritic type in headwater areas and a trellis type farther downstream. Several of the larger streams, including the Clinch River, flow through water gaps in the ridges.

Perennial springs are common to abundant near the bases of ridges underlain by the Knox Group. Only scattered and generally small perennial springs occur in other areas. During and soon after large rainfall events, wet-weather springs are common in gullies and other depressions. Some wet-weather springs flow from areas of saturated soil that have diameters of several meters to several tens of meters.

Sinkholes are common in areas underlain by the Knox Group and are abundant in the Freels Bend area of the Clinch River. Sinkholes are uncommon in most other areas. The largest sinkhole on the ORR, however, may be one atop Haw Ridge adjacent to State Highway 95; this depression is about 150 m long, 75 m wide, and 20 m deep in dolostone of the Rome Formation; it contains a swallow hole near its western edge. Only a few sinkholes show evidence of collapse. A few caves occur in the Knox Group on Copper Ridge and, reportedly, near the K-25 site. Also, at least a few swallow holes and resurgent springs occur in the Chestnut Ridge area of the Knox Group (Ketelle and Huff 1984, pp. 131-135).

## 1.2 GEOLOGIC SETTING

Rock units on the ORR range from Cambrian to Mississippian in age. The Rome Formation, which is 120 to >450 m thick, is of Cambrian age and underlies Haw Ridge, Pine Ridge, and an unnamed ridge between Pine Ridge and East Fork Ridge. The Rome generally consists of variegated shale, siltstone, and sandstone but includes massive dolostone beds in some areas. The overlying Conasauga Group of Cambrian age is about 520 m thick and crops out in Melton Valley, Bear Creek Valley, and smaller areas near the K-25 site. Most of the Conasauga Group consists of alternating sequences of shale, siltstone, and thin-bedded limestone. However, the Maynardville Limestone at the top of the Conasauga Group is about 100 m thick and consists of massively bedded limestone and dolostone. The Knox Group is Upper Cambrian to Lower Ordovician in age and is about 750 m thick. It consists mostly of massively bedded dolostone, siliceous dolostone, and chert. The Knox Group crops out on Copper Ridge, Chestnut Ridge, and Blackoak Ridge. The overlying Chickamauga Group is about 530-580 m thick and consists of maroon shales separated by gray limestones in Bethel Valley. In East Fork Valley, the Chickamauga Group consists of gray limestone and shaley limestone with thinner shale units. The Ordovician-age Reedsville Shale and Sequatchie Formation, the Silurian-age Rockwood Formation, the Devonian- to Mississippian-age Chattanooga Shale, and the Fort Payne Formation of Lower Mississippian age occur only in a syncline on East Fork Ridge.

The ORR portion of the Valley and Ridge Province consists of southeast-dipping rocks within several major thrust sheets. The Copper Creek thrust fault comes to the surface on Haw Ridge, and several branches of the Whiteoak Mountain thrust fault occur in the valley between Pine Ridge and East Fork Ridge. Northwest of this area, the rocks are a part of the Kingston thrust sheet.

Along both the Copper Creek and Whiteoak Mountain faults, the Rome Formation has been overthrust onto the Chickamauga Group. The rock layers strike about N55°E on an average. The dips are commonly about 20° in Melton Valley, 35° in Bethel Valley, and 45° in Bear Creek Valley but have a large range (10-85°) near the K-25 site. Also, dips in Melton Valley decrease with increasing depth and distance from a thrust fault. Small faults and folds are common, especially in the Rome Formation and the Conasauga Group.

A large majority of the fractures in the rocks constitutes a single cubic system (Sledz and Huff 1981). One fracture set is formed by bedding planes; the other two fracture sets are joints and are approximately parallel to the strike and dip of the rock layers. The dip of the joints is commonly about 60-80° on outcrops. These three fracture sets may be assumed to occur in all areas, and other extension and shear sets may also be present. Fractures may be abundant on outcrops, and Dreier et al. (1987, pp. 54-55) measured an average fracture density of about 200/m in saprolite of the Conasauga Group. At the other extreme, Sledz and Huff (1981, pp. 44-55) measured a minimum fracture density of 5/m on rock outcrops. Fewer fractures are visible in cores at deeper levels where, as noted by Haase et al. (1985, pp. 63-67), many fractures in sandstone and limestone are filled with secondary minerals. The spacings of pervious fractures below the water table are described in this report.

### 1.3 HYDROLOGIC SETTING

Average annual precipitation in the Valley and Ridge Province has a larger range than in the rest of Tennessee because of the topographic influences of the Cumberland Plateau and the Great Smoky Mountains; the range in most of the Province is 1020-1370 mm. Precipitation for the Oak Ridge area is near the upper end of this range. Normal precipitation for the Oak Ridge station of the National Weather Service was about 1350 mm/year for the

period 1951-88. The mean annual precipitation for the same station in 1977-88 was 1270 mm, and the mean annual precipitation for this period at a gage in WAG 5 near ORNL was 1190 mm.

The wettest months are January through March, and the driest months are August through October; in these periods, mean monthly precipitation at the Oak Ridge station is 130-160 mm and 74-96 mm, respectively. The monthly extremes for the Oak Ridge station are 340 mm for January 1954 and 13 mm for August 1953 (NOAA 1974, p. 378). The average frequencies of occurrence for various precipitation intensities over periods of 30 min to 24 h are shown by McMaster (1967, Fig. 3). Droughts lasting 7 d occur about 17% of the time, but droughts lasting 15 d occur only 1.8% of the time (McMaster 1967, Fig. 5).

Mean annual runoff for streams on the ORR, not including water imported from the Clinch River for use by the DOE facilities, is about 590 mm, which is the average for nearby basins with the same annual precipitation (May et al. 1970, Table A-3). Average quarterly runoff (McMaster 1967, p. 10) as a percentage of mean annual runoff is 17% for October-December, 49% for January-March, 23% for April-June, and 11% for July-September.

The average consumption of water by evapotranspiration on the ORR can be measured as precipitation minus mean annual runoff and is about 760 mm. Pan evaporation studies at Norris Dam [Tennessee Division of Water Resources (TDWR) 1961, p. 18] show that about 75% of the evapotranspiration occurs in a 6-month period from April through September. A water balance graph for Rogersville, Tennessee, shows that potential evapotranspiration exceeds precipitation for 5 months, from May through September, and that the main period for the replenishment of this soil water deficit is October 1 to November 10 (TDWR 1961, Fig. 4). Most recharge to the water table occurs in the period December to April when precipitation is above average, soil water content is high, and evapotranspiration losses are low.

## 2. OVERVIEW OF THE CONCEPTUAL MODEL

The subsurface flow system on the ORR consists of a stormflow zone, which approximately corresponds to the root zone of vegetation, a vadose (unsaturated) zone, and a groundwater zone. The water table generally occurs near the regolith and bedrock contact; the geometric mean of regolith thickness in the ORR aquitards is 3.9 m, and the geometric mean of depth to water in October is 4.1 m (Moore 1988, pp. 19-20, 60-61). The stormflow zone is missing on urbanized and barren lands, and it is disrupted in areas with trench-fill materials, which are more permeable than undisturbed soils. Elsewhere, the stormflow zone is thicker and more permeable in forested than in grassy areas. The average permeability of the vadose zone and the groundwater zone is larger in areas underlain by the Knox aquifer than in areas of the ORR aquitards (Fig. 2). The Knox aquifer consists of the Knox Group and the underlying Maynardville Limestone of the Conasauga Group. The ORR aquitards include all other geologic units, although a few massive limestone or dolostone layers in these units have some characteristics of the Knox aquifer in some areas.

In vegetated areas, the vertical permeability of the stormflow zone is larger than the 1-h precipitation intensity (7.6 cm for 100-year recurrence interval; McMaster 1967, p. 8), and nearly all rainfall is absorbed. Also, the stormflow zone is much more permeable than the vadose zone. Large precipitation events produce a transient perched water table in the stormflow zone, and water is then transmitted downslope to the streams. However, some water also percolates down to the water table whenever there is infiltration or a perched water table in the stormflow zone.

Overland runoff in the ORR occurs as a result of precipitation on impermeable surfaces (mainly urban features), water bodies, and saturated soils. In natural areas, nearly all

overland runoff occurs where the stormflow zone has overflowed. This condition is uncommon in areas of the Knox aquifer, but is common and extends over large areas in the ORR aquitards. The main difference is apparently the larger permeability of the vadose zone in areas of the Knox aquifer; water percolates to the water table at a faster rate, and the stormflow zone overflows in only a few favorable locations after the largest precipitation events. In contrast, depression water storage, which can be seen in valley grasslands of the ORR aquitards after large rainfall events, indicates a saturated stormflow zone over relatively large areas, and wet-weather springs at high elevations indicate a

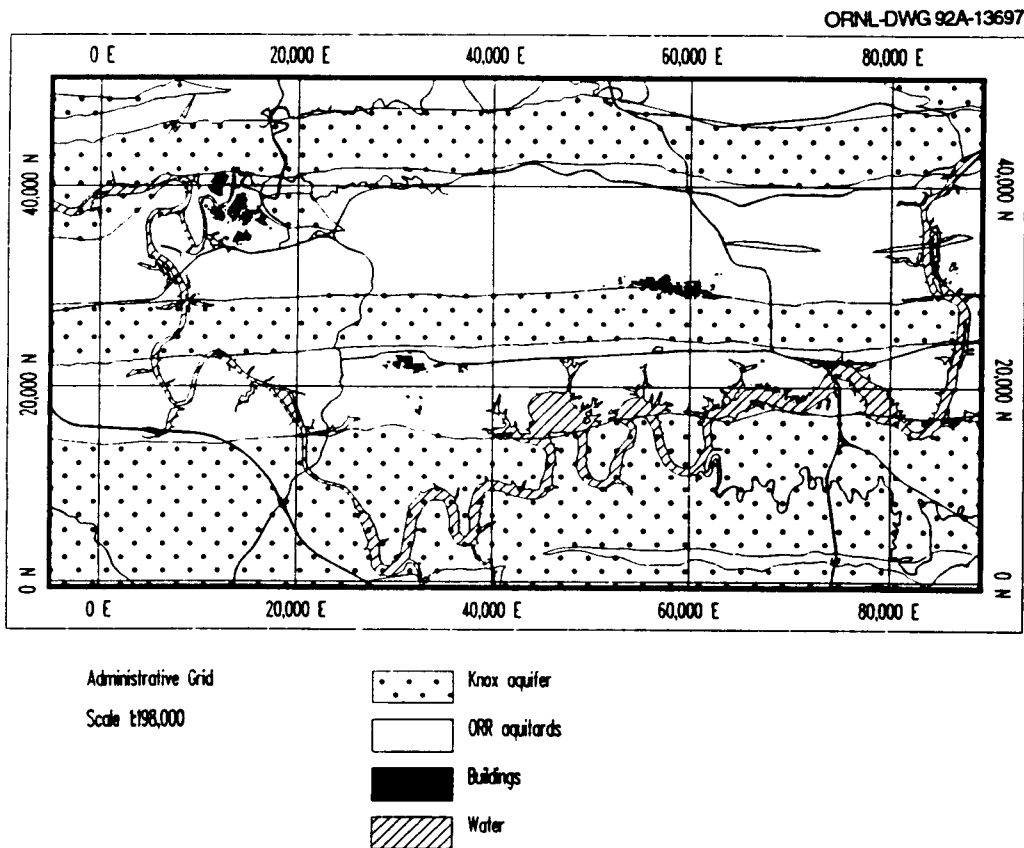


**Fig. 2. Locations of the Knox aquifer on the Oak Ridge Reservation.**

filled stormflow zone in the downslope gullies. Streamflow hydrographs for Ish Creek (Knox aquifer) near ORNL show overland runoff after only one storm event in the 1990 water year. Peak streamflow during other rainfall events apparently consisted of discharge from the stormflow zone. In contrast, peak streamflow during all rainfall events of the 1990 water year in the headwaters of Melton Branch (ORR aquitards) near ORNL consisted almost entirely of overland runoff (Moore, 1992, p. 392).

The occurrence of a perched water table in the stormflow zone shows that the local rainfall intensity and infiltration rate exceeded the percolation rate in the vadose zone. During most rainfall events, a perched water table forms in only a part of a drainage basin. Stormflow discharge to the streams thus occurs from partial contributing areas except after large rainfall events. Nevertheless, a stormflow monitoring tube on a drainage divide (an unfavorable location) in the headwaters of Melton Branch (ORR aquitards) had inflows of water during seven rainfall events between November 8, 1989 and June 6, 1990.

Discharge rates from the stormflow zone (measured as streamflow) depend upon contributing area, length of flowing streams, saturated thickness, hydraulic conductivity, and hydraulic gradient. These factors may be nearly the same throughout the ORR because peak discharge rates per unit drainage area are similar for the Melton Branch headwaters and Ish Creek (Solomon et al. 1992, p. 3-11). As discussed below, however, the other characteristics of flow in these streams are different.

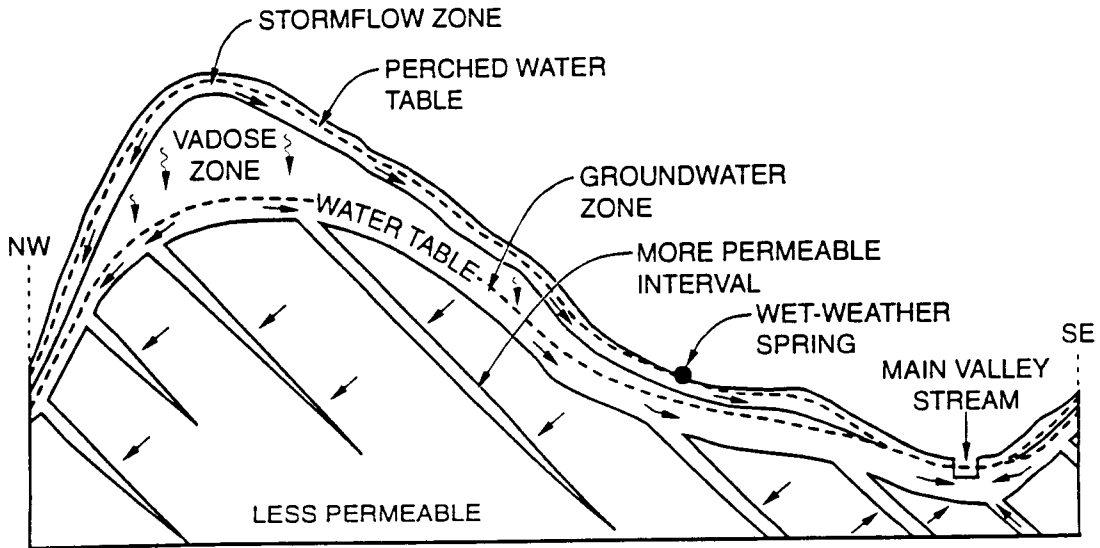
During the nongrowing season in the Melton Branch basin, overland runoff is followed by stormflow discharge after 1-2 d of recession and then by discharge from the groundwater zone after about 10 d of recession (Moore 1992). During the growing season, however, base flows are poorly sustained because of the consumption of water in the stormflow zone by evapotranspiration. Streamflow hydrograph peaks, which are mostly overland runoff, are

followed by steep recessions for periods of 1-3 d, and natural flows thereafter are near zero until the next precipitation event. In the Ish Creek basin, however, streamflow hydrographs are nearly the same throughout the year. Streamflow peaks of various sizes represent different contributing areas for stormflow discharge and are followed, after about 5-10 d of recession, by slowly decreasing discharge from the groundwater zone.

The water table is <1-2 m deep near perennial stream channels but is about 5-15 m deep beneath ridges in the ORR aquitards and 10-75 m deep beneath ridges in the Knox aquifer. Because of the larger permeability of the vadose zone, about 3.3 times more recharge occurs in areas of the Knox aquifer than in areas of the ORR aquitards (Solomon et al. 1992, p. 3-16). For this reason, the average annual fluctuation of water levels in wells is about 1.5 m in the ORR aquitards and 5.3 m in the Knox aquifer. Most groundwater is discharged in the channels of perennial and ephemeral streams.

The groundwater zone of the ORR can be divided into the water-table interval, the intermediate interval, the deep interval, and the aquiclude. The boundaries between one interval and another generally occur at different levels in different areas, depending on the local topography, lithology, and structure. The water table interval consists of a permeable fracture network in which most groundwater flows in the direction of the maximum hydraulic gradient and discharges into the closest stream (Fig. 3). The intermediate interval consists of a few relatively permeable fracture networks separated by thicker intervals of relatively impermeable rocks. Most groundwater in the intermediate interval flows in the strike direction of the rocks and discharges into cross-cutting tributary streams. The remainder flows downdip and then seeps upward through less permeable fractures and discharges into main-valley streams (Fig. 3).

**Dip Section**



**Strike Section**

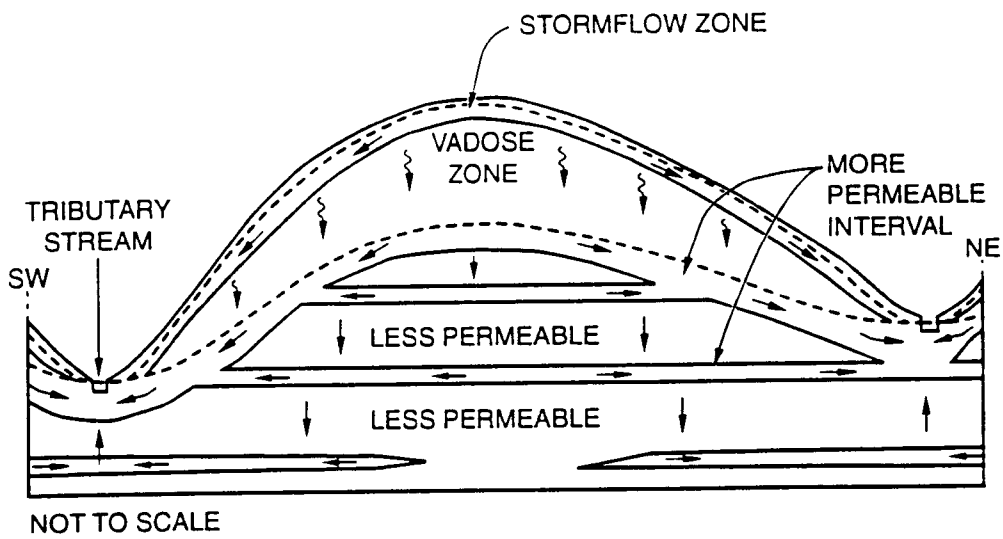


**Fig. 3. Hydrogeologic zones and directions of water flow on the Oak Ridge Reservation.**

Water flux decreases with depth, and the deep interval in the groundwater zone is characterized by a sodium bicarbonate water type rather than the calcium or calcium-magnesium bicarbonate water type that occurs in the water table and intermediate intervals. The top of the deep interval may occur at depths of 20-30 m in the ORR aquitards but at depths of 30-90 m in the Knox aquifer. Water in the deep interval probably seeps upward through low-permeability fractures and mixes with larger quantities of the calcium bicarbonate water because sodium bicarbonate springs have not been found on the ORR.

The aquiclude occurs at depths of 180-240 m in Melton and Bethel valleys and may occur below depths of 200-400 m in Bear Creek Valley. Water in the aquiclude is a sodium chloride type, and the content of total dissolved solids is 2000-275,000 mg/L. This water is essentially stagnant because there are no known sodium chloride springs on the ORR.

The average rate of groundwater discharge to streams is small and is only about  $120 \text{ L min}^{-1} \text{ km}^{-2}$  in areas of the Knox aquifer and  $40 \text{ L min}^{-1} \text{ km}^{-2}$  in areas of the ORR aquitards (Solomon et al. 1992, p. 3-19). Some fractures, mostly in the Knox aquifer, have been enlarged by solution and physical erosion to form cavities. These cavities are almost always filled or partly filled with sediments. The cavities may have formed in the geologic past, during a period with a wetter climate than that of the present.

Some springs and some wells that intercept open cavities in the Knox aquifer have large yields of water (Solomon et al. 1992, p. 3-21). Near the cavity systems, all groundwater probably flows toward the cavities, which act as drains or underground conduits. Nevertheless, most wells in the Knox aquifer yield  $<4 \text{ L/min}$  of water, as do nearly all wells in the ORR aquitards.

### 3. PHYSICAL CHARACTERISTICS OF THE GROUNDWATER ZONE

The permeability of the unfractured rock matrix on the ORR is insignificant, and essentially all groundwater flow occurs in fracture networks that form thin but relatively permeable intervals. The average hydraulic conductivity of the relatively permeable intervals is >100 times larger than that of the thicker, relatively impermeable intervals (Solomon et al. 1992, pp. 3-19 and 3-20). For these conditions, according to the tangent law for heterogeneous systems (Freeze and Cherry 1979, p. 173), lateral flows of groundwater occur only in the relatively permeable intervals. Flows in the relatively impermeable intervals occur along connecting fractures, and these flow paths are nearly orthogonal to the permeable intervals.

#### 3.1 PRIMARY POROSITY AND PERMEABILITY

The total porosity of rocks is commonly measured in a laboratory as the ratio of the weight of a dried sample to the weight of the same sample after saturation in a vacuum. Ten rock samples from the Joy-1 corehole at depths of 47-870 m had a range in total porosity of 0.0046-0.019; the arithmetic mean porosity was 0.0096 (de Laguna et al. 1968, p. 22). There is no apparent relationship between porosity and depth. Other samples from this core showed an average porosity of 0.022 for limy shale, 0.009 for sandstone, and 0.003 for limestone (Diment and Robertson 1963, p. 5039). The horizontal hydraulic conductivity for 12 samples from the same core had a range of  $1.1 \times 10^{-8}$  to  $4.2 \times 10^{-7}$  m/d, and the geometric mean of these data was  $8.7 \times 10^{-8}$  m/d. The relatively small range in hydraulic conductivity of the core samples, the differences in lithology, and the large range in depth suggest that these data may be representative of fresh, unfractured rock.

### 3.2 POROSITY OF REGOLITH, SAPROLITE, AND FRACTURES

The total porosity of regolith and saprolite is commonly calculated as 1.0 minus bulk density, which is the ratio of the density of the dry sample to the average density of nonmetallic minerals ( $2.65 \text{ g/cm}^3$ ). Based on this method, regolith in Walker Branch watershed (Knox aquifer) near ORNL has a mean porosity of 0.30 (Peters et al. 1970, p. 85), and shaley saprolite in trench walls at WAG 6 (ORR aquitards) near ORNL has a mean porosity of 0.50 (Davis et al. 1984, p. 55). These results show that the porosity of regolith and saprolite is approximately the same as that of unconsolidated sediments. Thus, the reservoir for contaminant storage by matrix diffusion may be much larger near the water table than at deeper levels.

Effective porosity is the decimal fraction of rock volume that permits fluid flow. Specific yield is the ratio of the volume of water that drains by gravity to the total volume of rock. If only the water in pervious fractures drains by gravity, effective porosity and specific yield are nearly the same. Fracture aperture can be calculated from transmissivity (Appendix A.1), and a one-dimensional measure of effective porosity is the ratio of aperture to fracture spacing. A cumulative probability graph (Fig. 4) shows that the geometric mean of fracture aperture is 0.12 mm. Average orthogonal fracture spacing, as is discussed later, is about 35 cm (the geometric mean of the lognormal population), and effective fracture porosity is thus about  $3.5 \times 10^{-4}$ .

Storativity is calculated from aquifer-test data and is nearly the same as specific yield under unconfined conditions. Under confined conditions, as occur at deeper levels (Moore 1988, p. 48), storativity may represent chiefly the elasticity of fracture walls. Nevertheless, the water yield produced by changes in fracture aperture may be nearly the same as the yield produced by drainage. Twenty-six storativity values, calculated from

observation-well data during aquifer tests on the ORR, have a geometric mean of  $7.6 \times 10^{-4}$ . This result is larger but not substantially larger than that of the average effective porosity, above. Also, the average specific yield, which was determined by hydrograph analysis (Appendix A.2), for the permeable zone at the water table in the headwaters area of Melton Branch (ORR aquitards) is  $2.3 \times 10^{-3}$  (Moore 1992, p. 394). This result is larger than average storativity and average effective porosity, but drainage from the regolith, including delayed drainage, may increase the specific yield near the water table.

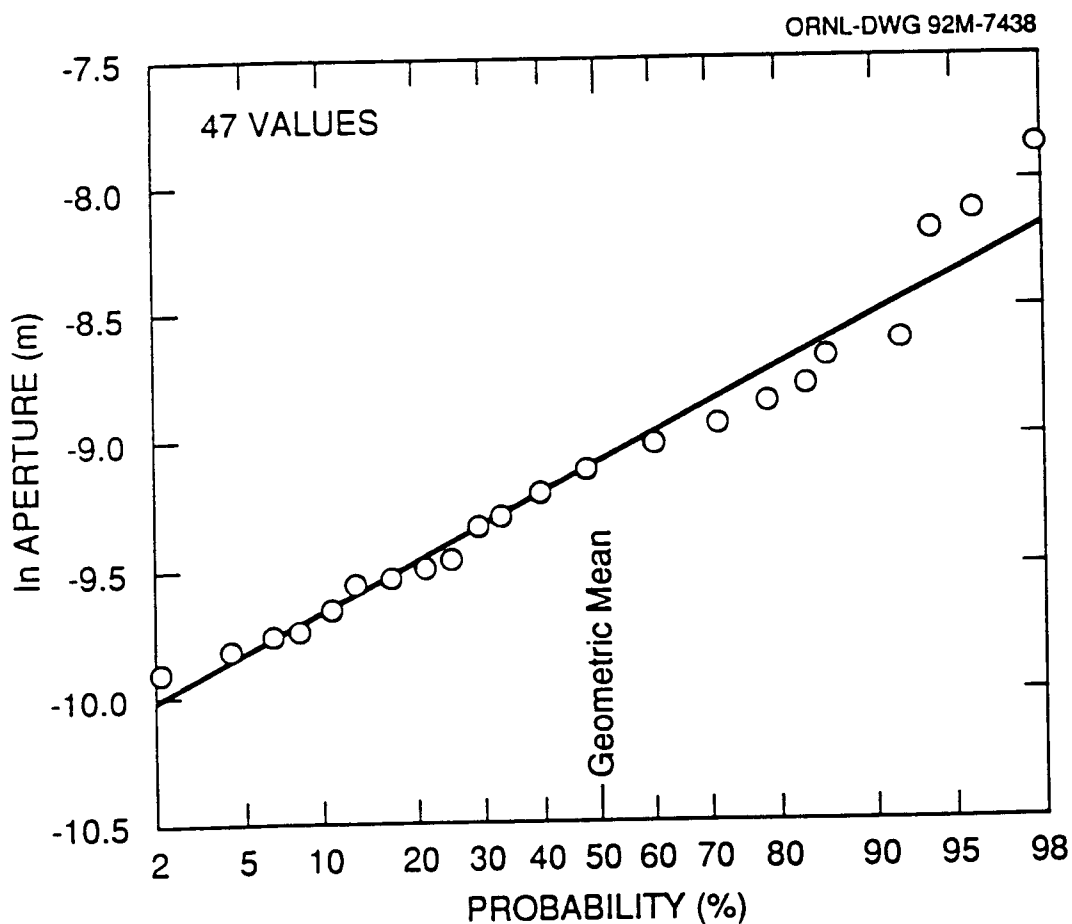


**Fig. 4. Cumulative probability graph of fracture apertures calculated from transmissivity data.**

### 3.3 OCCURRENCE AND SIGNIFICANCE OF PERVIOUS FRACTURES

Groundwater flow is assumed to occur through orthogonal sets of pervious, planar fractures, and a permeable interval at any level is assumed to consist of an intersecting network of pervious fractures. One permeable interval occurs nearly everywhere at the water table (Fig. 3). The hydrologic importance of flow at this level was first postulated by Webster (1976, pp. 15-16) and Webster and Bradley (1987, pp. 29-30, 79). There is now considerable evidence that this concept is correct (Solomon et al. 1992, pp. 3-17 to 3-19).

Other information about the permeable intervals and about the pervious fractures in these intervals was recently obtained from borehole flowmeter surveys (Appendix A.3). The electromagnetic borehole flowmeter, recently invented by the Tennessee Valley Authority, produces an absolute measurement of the flow rate up or down a well at a selected depth position; the relative change in flow rate between two depth positions shows the presence or absence of a pervious fracture in the interval (Moore and Young 1992, p. 3). If a well has no natural flow, flow is induced by pumping or injecting water. Borehole flowmeter surveys indicate that the mean thickness of the permeable intervals is about 1.5 m, and the range is 0.25-4.6 m. However, the maximum thickness of the permeable intervals is biased because about 65% of the wells have screen lengths of 3.0 m. The standard deviation of data in the lower part of the range indicates that the 5-95% probability range for the thickness of permeable intervals is 0.25-7.5 m.

In detail, the borehole flowmeter surveys of wells show 1-3 pervious sections and 0-2 impervious sections within a permeable interval (Fig. 5). These surveys also show a nearly linear change in flow rate within a pervious section and abrupt changes to a nearly constant flow rate at the top and bottom of a pervious section. These characteristics apparently indicate that each pervious section consists of a single fracture with a uniform

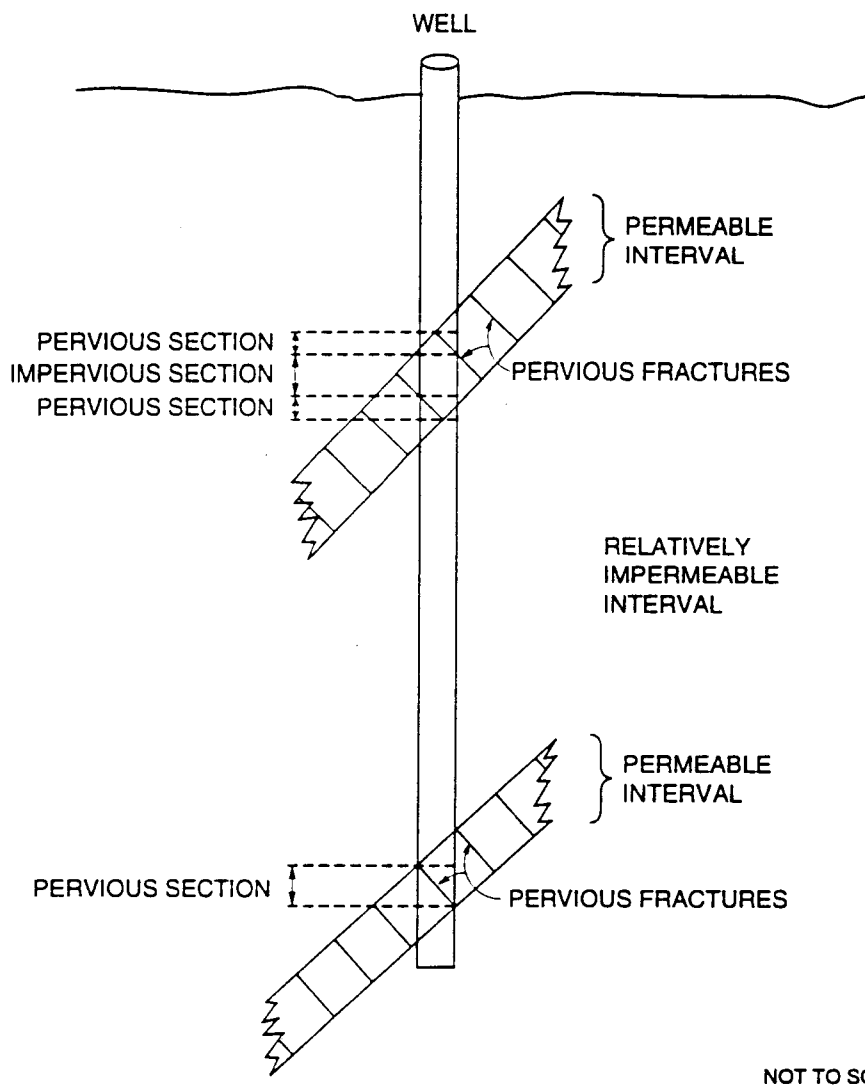


**Fig. 5. Diagram showing relationship of pervious fractures to pervious sections and permeable intervals in a well.**

hydraulic conductivity. Pervious fractures, as shown later, have a range in hydraulic conductivity that includes >2 orders of magnitude, and it is unlikely that multiple fractures would produce a constant change in flow rate across each of many pervious sections. If this interpretation is correct, the thickness of a pervious section in a well is an indication of the minimum width and dip of the fracture, and the thickness of an impervious section between two pervious sections is an indication of the maximum fracture spacing.

The thickness (vertical extent) of pervious sections within the permeable intervals has a range of 0.24-3.5 m in the borehole flowmeter surveys. These data are lognormally distributed, and the geometric mean is 0.67 m. A classification of the data shows that 40% of the pervious sections within 3.0 m of the water table have a thickness of >1.2 m, but none of the sections >6.1 m below the water table are thicker than 1.2 m. This difference might be caused by fracture propagation at shallow depths, but there is some evidence, as described below, that sections with a thickness of >1.2 m have different orientations and smaller apertures. At depths >6.1 m below the water table, the geometric mean for the thickness of pervious sections is 0.49 m, and the range from the mean minus one to the mean plus one standard deviation is 0.30-0.76 m. This range shows that fractures have dips of at least 61-78°; pervious sections thicker than 1.2 m represent fractures that have dips of at least 82°. The dips of fractures that terminate within the wells may be larger than these values.

If fractures are assumed to terminate at the edges of the boreholes and if fracture dip is 61-82°, fracture width has a range of 0.24-4.0 m. Although most fractures extend beyond the boreholes, this range includes more than an order of magnitude, and nearly all fractures on rock outcrops are <4 m wide. Thus, the calculated range for fracture widths probably includes most of the actual range.

The orthogonal spacing of fractures can be estimated from fracture dip, well diameter, and the thickness of low-permeability sections within the permeable intervals (Fig. 6). Flowmeter survey data show that the thickness of low-permeability sections in piezometer wells is lognormally distributed. The geometric mean of thickness in wells with two or more pervious sections is

ORNL-DWG 92M-1660R

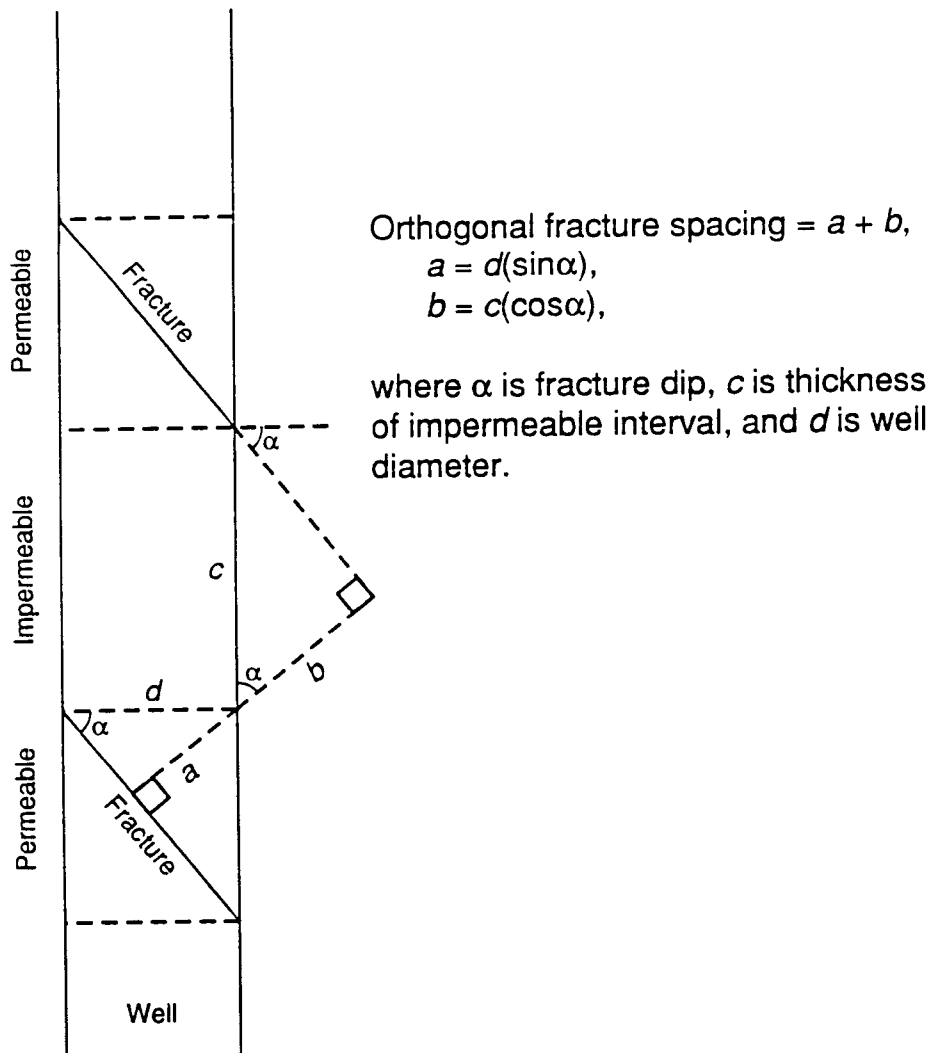


Fig. 6. Diagram showing geometry for the calculation of orthogonal fracture spacing.

is 0.49 m; this value might be smaller than the true average because some wells that intercept only one permeable fracture might have intercepted two fractures if the screen had been longer. The geometric mean of thickness for the thickest low-permeability interval in all wells is 0.85 m; this value may be larger than the true average because some wells would not have intercepted a second fracture with a longer screen. If the thickness of low-permeability sections is 0.49-0.85 m, well diameter is 16.5 cm, and fracture dip is 61-82°, orthogonal fracture spacing has a range of about 23-56 cm; the more steeply dipping fractures have the closest spacing. If some fractures terminate within the wells and thus have steeper dips, minimum fracture spacing may be about 16 cm.

The ORRHAGS geologic study has identified two fracture sets that occur throughout the ORR and two other sets that occur in parts of the area. One fracture set that occurs throughout the ORR trends 40-65°NE and approximately parallels the strike of the rock layers; the other set trends 30-50°NW and is approximately parallel to the dip of the rocks. The two fracture sets that occur in only parts of the ORR have trends of 5°NE and 65-70°NW.

Previous studies have shown that water level drawdown patterns are elongated in the northeast-southwest (strike) direction during pumping tests and that a tracer arrives first in a well that is northeast or southwest of the injection well (Webster 1976, pp. 15-16; Webster and Bradley 1987, pp. 26-30). However, Webster and Bradley (1987, p. 27) also described first arrivals and maximum concentrations of tracers at wells in the direction of maximum hydraulic gradient (normal to the strike of the rock layers) for two tracer tests at the water table. During these tests and in one other test (Davis et al. 1984, p. 77), the tracer eventually appeared in all observation wells that had a lower potentiometric head than that in the injection well.

Elliptical water-level drawdown patterns and the results of tracer tests on the ORR can be explained if the fractures near the water table have a number of different orientations but if a large majority of fractures at deeper levels are strike parallel. However, the continuity of groundwater flow paths at any level requires at least some cross-cutting, intersecting fractures because all fractures in a parallel set have a finite length. Also, the downdip flows of small amounts of water (Fig. 3) require a few dip-parallel or bedding-plane fractures. The occurrence of two or more intersecting fracture sets in the permeable zone near the water table apparently produces good continuity for groundwater flows because this zone is nearly ubiquitous; the widespread continuity probably results from a large groundwater flux and multiple, alternative flow paths. The eventual appearance of a tracer in wells that have a large difference in the azimuth from an injection well may occur only near the water table.

About 45% of the wells surveyed with the borehole flowmeter (Melton and Bear Creek valleys; ORR aquitards) intercept two or more pervious fractures within a single permeable interval; about 2% intercept three pervious fractures. There is no significant difference in the percentages of wells that intercept multiple fractures at depths of <3.0 m below the water table and at depths of >6.1 m below the water table. Thus, the flowmeter surveys do not show that fracture spacing is different near the water table than at deeper levels. The specific yield of the permeable layer near the water table is apparently larger than that of deeper permeable intervals, but drainage from the regolith may account for this difference. Also, the different trends of fractures near the water table do not necessarily indicate a closer fracture spacing.

The permeable zone at the water table has a configuration that is determined by depth rather than by the orientation of the rock layers, and most or all of the fractures are nonstratiform. In the intermediate and deep intervals of the groundwater zone, most of the strike-parallel fractures within the permeable intervals probably are stratiform. These fractures may terminate or become much less permeable at some bedding planes and fracture intersections. The cross-cutting, intersecting fractures within the permeable intervals apparently have a lower spatial density, as is discussed later, and may or may not be stratiform.

The average hydraulic conductivity of the relatively impermeable intervals in the intermediate part of the groundwater zone is about four orders of magnitude larger than that of fresh, unfractured rock but it is about two orders of magnitude smaller than that of relatively permeable intervals (Table 1). This small but enhanced permeability indicates smaller fracture apertures or a sparse fracture network, and these fractures probably are not stratiform. At a few locations, especially in areas of the Knox aquifer, the fractures that connect two permeable intervals might permit large groundwater flows. However, small rates of upward or downward seepage over broad areas might be adequate to explain solution cavities and other permeable intervals at depths of 10-100 m or more below the valleys in some areas of the ORR.

Relatively permeable intervals probably represent the segments of a preexisting fracture network where apertures have been enlarged by solution along flow paths that lead toward discharge locations for groundwater. The reason why pervious fractures occur in only a few rock layers is uncertain. However, a combination of (1) slow uplift, erosion, and slump, and (2) earth tides and cyclic fluctuations in hydraulic pressure might have caused preferential fracture propagation in some relatively brittle rock layers. Fracture propagation eventually would have produced a connected fracture network.

Karst features generally occur in thick to massive layers of relatively pure limestone and dolostone where the preexisting fractures are likely to have been longer and better connected (Ford and Williams 1989, pp. 30-38). This principle probably explains the cavity systems in the Knox aquifer. In the ORR aquitards, however, there is no apparent relationship between fracture permeability and either geologic unit or lithology.

Fracture enlargement by solution is aided by a large water flux. The multiple orientations of pervious fractures near the water table may occur because the groundwater flux is a maximum at this level and because the shortest path length (maximum hydraulic gradient) to a nearby stream may occur in any direction. In the intermediate and deep groundwater intervals, aperture enlargement probably occurred in networks produced by the longer and better connected fractures. Within these networks, strike-parallel fractures represent the shortest flow path toward cross-cutting tributary streams, and dip-parallel fractures represent the shortest flow path toward main-valley streams.

The combined results from injection tests (Appendix A.3) and borehole flowmeter surveys in Melton Valley (ORR aquitards) show an apparent relationship between the groundwater flux and the average permeability and width of the fractures. The average hydraulic conductivity in the data, below, is nearly the same for fracture widths up to about 0.9 m but decreases for wider fractures. Average transmissivity increases with fracture width up to a width of about 0.9 m but is nearly constant for wider fractures. These results apparently show that fracture width is proportional to flow rate up to a width of about 0.9 m. Also, however, the widest fractures have a nearly constant transmissivity, and widths >0.9 m are apparently unnecessary for the maximum groundwater flux.

Fracture width (m)	Number of values	Geometric mean of hydraulic conductivity (m/d)	Geometric mean of transmissivity (m <sup>2</sup> /d)
0.24-0.30	10	0.15	0.046
0.30-0.61	26	0.15	0.066
0.61-0.90	20	0.15	0.10
0.91-1.22	8	0.087	0.091
>1.22	8	0.038	0.086

### 3.4 FRACTURE PERMEABILITY

As discussed in Solomon et al. (1992, pp. 3-19 to 3-21), a cumulative probability graph of transmissivity data from slug tests (mainly) shows that the geometric mean of transmissivity for permeable intervals in both the water table and intermediate intervals of the groundwater zone is 0.23 m<sup>2</sup>/d. Classifications and comparisons of these and newly acquired data show several corrections and bounds for the transmissivity and hydraulic conductivity values. First, recent injection tests show that transmissivity values from slug tests are too large because the effect of borehole water storage on early water level data is ignored. For example, the geometric mean of transmissivity from a group of slug tests on piezometer wells in Melton Valley (ORR aquitards) is 0.36 m<sup>2</sup>/d, whereas the geometric mean value from more accurate injection tests on the same wells is 0.13 m<sup>2</sup>/d (Fig. 7). The similar slopes of the two probability plots show, however, that the standard deviation of the data sets is the same.

The calculation of the hydraulic conductivity of permeable intervals from slug tests assumes that the entire length of a well screen is water producing whereas the borehole flowmeter surveys show that the average vertical extent of a permeable interval (1.5 m) is smaller than the length of the screen in most wells. If both the transmissivity value and the vertical extent of the permeable interval are too large, which is generally the case, the

errors are compensating. Thus, for example, the geometric mean of hydraulic conductivity for a group of slug tests on piezometer wells in Melton Valley is 0.081 m/d, and the geometric mean of hydraulic conductivity from injection tests on the same wells is 0.12 m/d (Fig. 8); these two results are nearly the same.

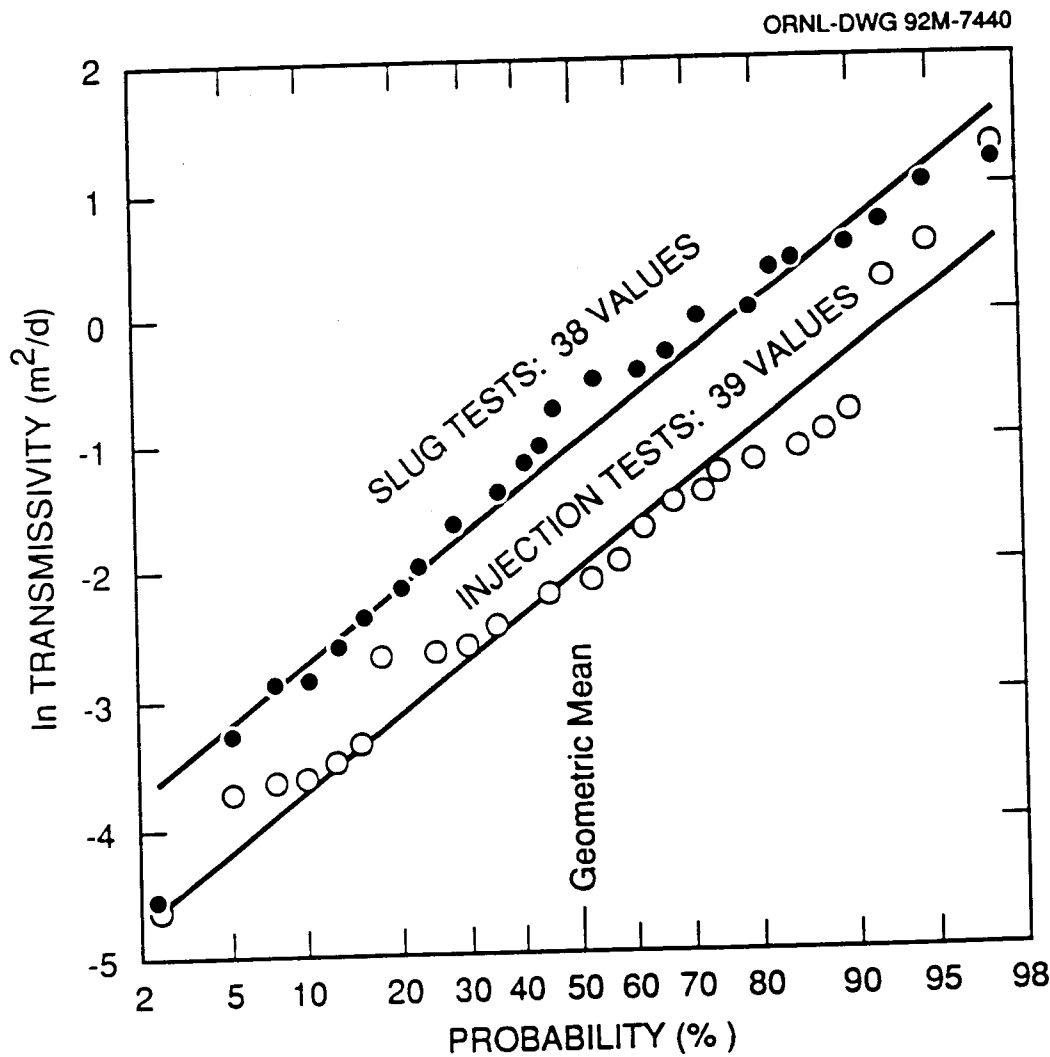


Fig. 7. Cumulative probability graphs for transmissivity data, which are calculated from slug tests and injection tests on the same wells.

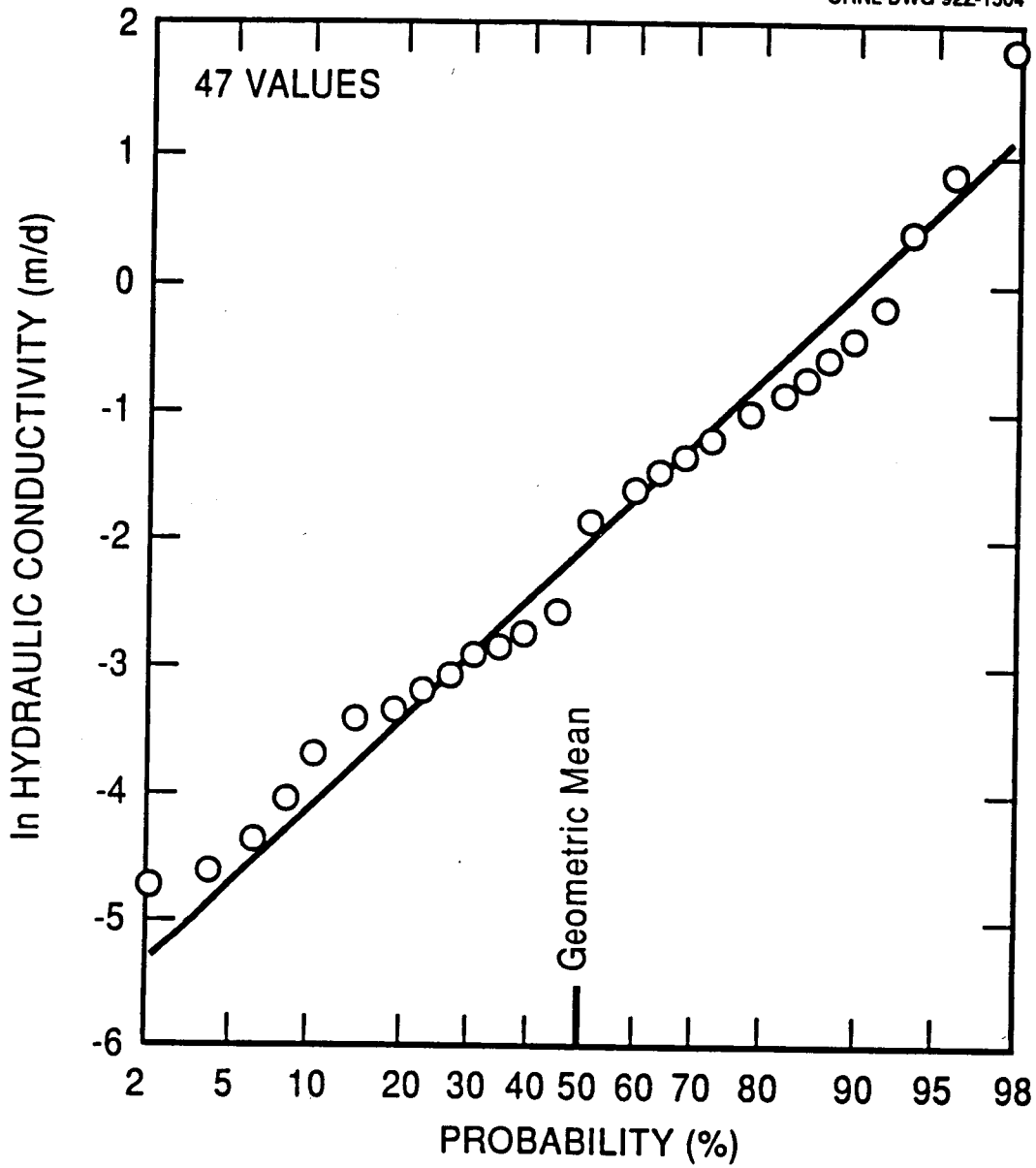


Fig. 8. Cumulative probability graph of hydraulic conductivity data for pervious fractures; data from injection tests and borehole flowmeter surveys.

As mentioned by Solomon et al. (1992, p. 3-20, 3-21) a data set from Bear Creek Valley (ORR aquitards) shows that transmissivity values are too small if screen length is shorter than the thickness of a permeable interval and that transmissivity values are too large if the length of the screen spans more than one permeable interval.

Screen length (m)	Number of values	Geometric mean of transmissivity (m <sup>2</sup> /d)
0.3-1.0	14	0.037
1.1-2.0	36	0.14
2.1-3.0	39	0.71
3.1-4.0	45	0.76
4.1-8.0	24	0.58
8.1-12.0	12	0.56
12.1-20.0	17	1.1
20.1-36.7	6	1.4
Population	207	0.41

The much larger average transmissivity for wells with screen lengths of >2.0 m indicates that the average vertical extent of a relatively permeable interval is about 2.0 m. The larger average transmissivity for screen lengths of >12 m shows that the average thickness of the rocks between two permeable intervals is about 12 m. For comparison, as mentioned previously, borehole flowmeter surveys show that the mean vertical extent of a permeable interval is 1.5 m. This result is essentially the same as that in the data above. Also, the differences in the depths of paired shallow and deeper wells are an average 11 m in Melton Valley and 12 m in Bear Creek Valley; this difference represents the vertical spacing between the shallowest and the next deeper permeable intervals in the ORR aquitards (Moore 1988, p. 46). The estimates of average vertical spacing between permeable intervals thus are nearly identical by two different methods.

A classification of the transmissivity data for Bear Creek Valley (ORR aquitards) by well depth, below, shows that the geometric means are approximately the same at depths of <100 m but are smaller at deeper levels.

Depth to top of well screen (m)	Number of values	Geometric mean of transmissivity (m <sup>2</sup> /d)
1.6-5.0	33	0.64
5.1-10.0	63	0.57
10.1-20.0	50	0.33
20.1-30.0	20	0.37
30.1-50.0	11	0.93
50.1-100	11	0.46
101-200	9	0.11
201-361	9	0.055
Population	207	0.41

In Bethel and Melton valleys, for comparison, Moore (1988, pp. 53-54) showed a decrease in the geometric mean of hydraulic conductivity below a depth of only 20-30 m. These results suggest that the average transmissivity of permeable layers in the deep groundwater interval is significantly smaller than the average transmissivity in the water-table and intermediate intervals but that the depth to the top of the deep interval has a range of at least 20-100 m. The results of injection tests do not show a difference in the average transmissivity of the water table and the intermediate intervals (Moore and Young 1992, p. 21), but most tests were made during dry periods when the saturated thickness of the water-table interval was in the lower half of the range.

The correction of transmissivity data for length of well screen is small on the ORR because screen length is larger than the thickness of a permeable interval in most wells. The corrected geometric mean of transmissivity for the data in Bear Creek Valley is 0.58 m<sup>2</sup>/d. However, Moore (1988, p. 48) showed that the geometric mean of hydraulic conductivity for fully developed water quality wells in WAG 6 near ORNL (ORR aquitards) was nearly twice as large as that of undeveloped piezometer wells in the same area.

### 3.5 RELATIONSHIP OF THE FRACTURES AND A CONTINUUM

The transmissivity and hydraulic conductivity of the fractures intercepted by a well determine the yield of the well, but the average properties of the continuum determine the groundwater flux. As described by Freeze and Cherry (1979, p. 73), "The analysis of flow in fractured rocks can be carried out either with the continuum approach. . . or with a noncontinuum approach based on the hydraulics of flow in individual fractures. . . . The continuum approach. . . is valid as long as the fracture spacing is sufficiently dense. . . . If the fracture density is extremely low, it may be necessary to analyze flow in individual fractures."

On the ORR, water level hydrographs for observation wells show that a plot of log stage versus time forms a straight line soon after a hydrograph peak. The slope of each line is a characteristic of the well, but the average recession slope of a group of wells is approximately the same as the recession slope for base flows on a plot of log streamflow versus time (Moore 1992, p. 392). This result indicates that low base flows are produced by discharge from the groundwater zone and that a rock volume of sufficient size approximates a continuum.

The geometric mean of transmissivity values measured with aquifer tests at wells is almost certainly smaller than the average transmissivity of the continuum. If the average spacing between relatively permeable intervals at shallow depths is 11-12 m, a hydrologic section that includes both the water table and intermediate intervals of the groundwater zone would contain several permeable intervals. Also, groundwater flow may occur in more than one direction in an intersecting fracture network, and a calculation of transmissivity for one planar set of fractures may underestimate that of the network.

About 85% of the injection tests on shallow wells in Melton Valley (ORR aquitards) showed recharge boundaries that are interpreted to represent the water contributions of pervious, intersecting fractures. If this interpretation is correct, the geometric mean of transmissivity calculated from the late data (water level data that show the effects of the boundary) should represent a larger volume of rock and may be close to the average transmissivity of the continuum. Cumulative probability graphs of early and late transmissivity data are somewhat irregular because of the small number of tests (Fig. 9). Nevertheless, straight lines through the plotted points are parallel, thereby indicating the same standard deviation for both data sets. The geometric mean of transmissivity for late data is  $0.65 \text{ m}^2/\text{d}$  and is 5-times larger than the geometric mean for early data ( $0.13 \text{ m}^2/\text{d}$ ). For comparison, Moore (1992, p. 394) used hydrograph analysis to calculate an average transmissivity of  $0.75 \text{ m}^2/\text{d}$  for the headwaters area of Melton Branch. The results of the comparisons suggest that it should be possible to measure the transmissivity of the continuum by any of the following methods: (1) analysis of observation well and streamflow hydrographs, (2) analysis of water level drawdown and recovery data in observation wells during pumping tests, or (3) analysis of late water-level data from pumping wells or injection wells.

Based on slug test results, the geometric mean of hydraulic conductivity for pervious fractures in the ORR aquitards is  $0.041 \text{ m/d}$  (Moore 1989, pp. 42-44); a corrected average value from a comparison of slug-test and injection-test data is  $0.061 \text{ m/d}$ . For a fracture spacing of  $0.35 \text{ m}$  (three fractures in a section of unit area), the average hydraulic conductivity for the continuum of permeable intervals is  $0.18 \text{ m/d}$ . If total transmissivity of the groundwater zone is an average  $0.75 \text{ m}^2/\text{d}$  (from hydrograph analysis), the total thickness of all permeable intervals is  $0.75/0.18 = 4.2 \text{ m}$ , and because the average thickness of a single

permeable interval is 1.5 m, there are an average 2.8 permeable intervals in the zone of active groundwater circulation. For comparison, if the intermediate interval of the groundwater zone extends to an average depth of 30 m (Moore 1988, pp. 43, 53-54) and if the average vertical spacing between permeable intervals is 11 m, there are 2.7 permeable intervals above the deep groundwater interval. These two results are nearly the same, suggesting that the calculated average hydraulic conductivity of the continuum is approximately correct. Although this value is applicable to only the permeable intervals, all lateral flows of groundwater occur in these intervals.

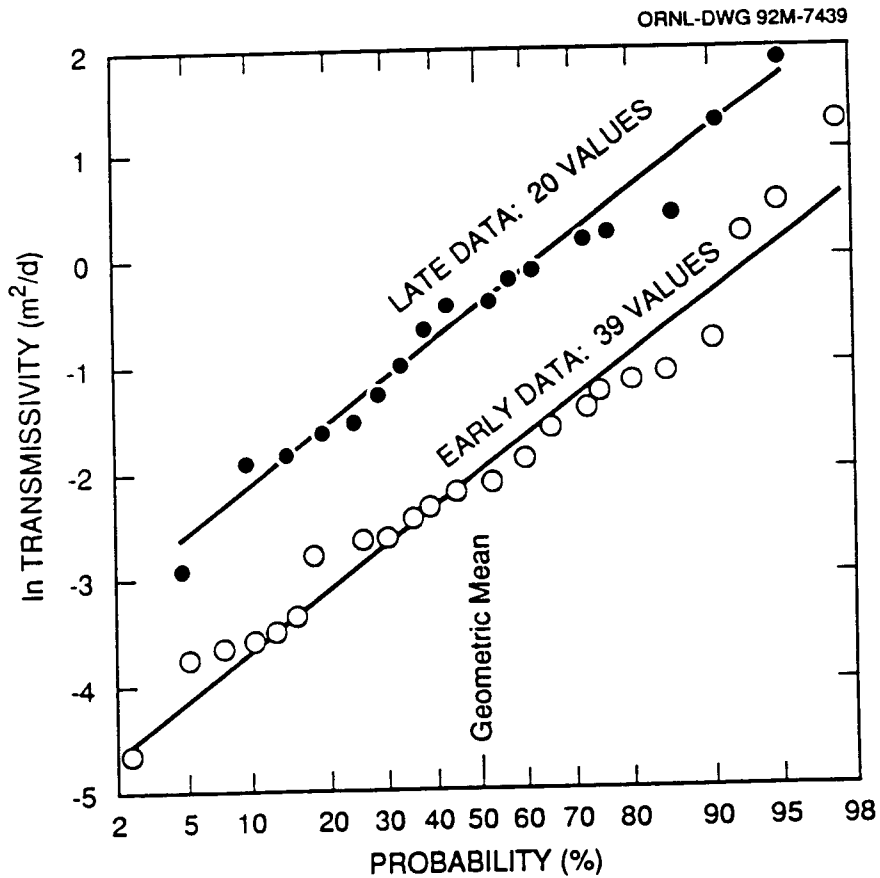


Fig. 9. Cumulative probability graphs of transmissivity values from early and late water-level data during injection tests.

### 3.6 GROUNDWATER FLOW PATHS

In the nonstratiform fracture network near the water table, most groundwater apparently flows in the direction of the maximum hydraulic gradient, but some flows also follow pervious fractures that trend along strike or downdip (Fig. 3). The hydraulic gradient is generally smaller along these alternative flow paths, but the hydraulic conductivity may be larger. In a few areas, linear flow paths occur where small folds and faults control the flow direction. Webster (1976, p. 8) summarized previous studies showing that some structures of this type persist along the strike of the rocks for distances of up to 300 m. Also, some cavities are nearly linear for distances of up to 1.8 km (Ketelle and Huff 1984, p. 133). In general, however, flow paths diverge near drainage divides and converge near streams. Also, most groundwater flow paths probably have staircase patterns with splits and joins at fracture intersections (Moore 1988, p. 66).

Stratiform fracture networks in the intermediate interval of the groundwater zone probably transmit most of the water that reaches this level along strike toward cross-cutting tributary streams (Fig. 3). The remainder flows downdip and then seeps upward through relatively impermeable rock layers toward discharge locations in main-valley streams (Fig. 3). Flow paths below the levels of the streams are longer and include longer segments in relatively impermeable rocks. There may be a consistent decrease in specific discharge with depth because the average hydraulic gradient decreases with length of flow path and because average permeability along the path decreases. Very little water circulates through the deep interval of the groundwater zone.

Nearly all water is discharged at the closest stream along the flow path. The main zone of groundwater circulation probably extends from the water table to a depth of only a few meters below stream level in the directions of the flow paths. All groundwater flow paths begin and end in the water table interval, and all

groundwater discharge results in a depletion of storage in this interval. Most downward seepage from the water table interval to the intermediate and deep intervals occurs beneath the ridges and hillslopes (Fig. 3); most upward seepage occurs in the valleys.

The water table interval fills to overflowing in a few locations after large recharge events and produces wet-weather springs in areas of the ORR aquitards. The average distance from a drainage divide to a stream at the time of the peak water table is about 90 m in the headwater area of Melton Branch (Moore 1992, p. 394). Later, during dry periods of the summer and fall, the average length of a groundwater flow path is about 200 m, and the maximum path length is about 400 m (Moore 1989, pp. 57-58). Part of the increase in path length during the growing season is caused by water losses to evapotranspiration where the water table is <2 m below the surface. During long droughts, the water table interval is partly drained. Small groundwater flows continue but may be captured by evapotranspiration near stream channels. In this case, groundwater is discharged to streams in only the lower part of the basin where the saturated interval above the level of the streams is thicker and where some pervious flow paths occur at deeper levels than in headwaters areas.

Less information is available on the characteristics of flow paths in the Knox aquifer because few studies have been made in these areas. Only some of the flow characteristics in areas of the ORR aquitards are applicable to the Knox aquifer. The directions of flow paths are probably the same, and flow rates in the Knox aquifer probably decrease greatly below the level of the streams. However, the water table is commonly deeper in areas of the Knox aquifer (30-75 m in some parts of Chestnut Ridge); the water table interval is less likely to fill to overflowing; and groundwater losses to evapotranspiration during the growing season may be smaller than in areas of the ORR aquitards. Also, a

transient, perched water table may form at various levels in the thick Knox regolith during recharge events and may produce wet-weather springs.

As noted previously, some fractures in the Knox aquifer have been enlarged to form cavity systems. Well yields and spring discharges from the largest of these cavities exceed 4000 L/min. Cavities also occur in the ORR aquitards but are less common. Except for areas near the K-25 site and the breeder reactor site, only about 10% of wells in the ORR aquitards intercept one or more cavities compared with about 40% of wells in the Knox aquifer (Moore 1988, pp. 31-32). There is about 3.5 times more recharge to and discharge from the Knox aquifer than for the ORR aquitards (Solomon et al. 1992, p. 3-15 to 3-16). This larger water flux probably explains both the more numerous cavities and the thicker regolith in areas of the Knox aquifer. Cavities are more common in the Chickamauga Group near the breeder reactor site, and near the K-25 site, cavities in the Chickamauga group are nearly as common as in the Knox aquifer.

Nearly all cavities in the Conasauga Group occur in the Maynardville Limestone and the Nolichucky Shale; most cavities in the Chickamauga Group occur in the Benbolt and Rockdell Formations and the Carters Limestone. These units contain thick to massive layers of relatively pure limestone. A few cavities in the ORR aquitards are large or transmit large quantities of water. For example, a cavity about 12 m high (vertical dimension) was intercepted by a well in Carters Limestone at the western edge of Whitewing scrapyard (ORNL WAG 11). Also, a cavity in the Benbolt Formation at the ORNL Main Plant apparently transmits >1200 L/min of water from a losing reach of Whiteoak Creek about 800 m southwestward to the duck pond at the heavy ion research facility. Both of these cavities are nearly strike parallel as, apparently, are the cavities in the Knox aquifer.

#### 4. SUMMARY OF HYDROGEOLOGIC CHARACTERISTICS

Some hydrogeologic parameters in Table 1 have been discussed in this report. The values of other parameters are from recent reports (Moore 1988, 1989, 1992; Moore and Young 1992; and Solomon et al. 1992) and represent the best available information. Considerable progress has been made in understanding the hydrogeology of the ORR in the past 5 years, and the most recent reports generally contain the most reliable data and other information.

Only the average value is listed for most items in Table 1. Nearly all hydrogeologic data are lognormally distributed, and the average is the geometric mean. The ranges of data on the ORR include  $<1$  to  $>6$  orders of magnitude, and a parameter may be much larger or much smaller than the average in a locality. Also, some values have been calculated by different methods and compared whereas other data were acquired in one small area. Nevertheless, the values in the table are the best available for modeling and other calculations.

For the stormflow zone in Table 1, thickness is the observed depth of the root zone; the range in forest areas is supported by linear flow recessions in monitoring tubes that extend to a depth of 1 m. Infiltration rates were measured in one large-area test (WAG 6 near ORNL) for grassland and in about 65 double-ring infiltrometer tests for forest. Total porosity was measured in multiple samples at two locations near ORNL. Macropore porosity was measured during some infiltration tests. Specific yield, hydraulic conductivity, and discharge rate were determined by hydrograph analysis for Ish Creek and the headwaters of Melton Branch. Storage capacity is calculated from specific yield and average thickness. Average hydraulic gradient was measured on topographic maps.

For the groundwater zone in Table 1, thicknesses, total porosity, fracture porosity, fracture aperture, hydraulic conductivity of the rock matrix, transmissivity of relatively permeable intervals, and transmissivity of the continuum values are discussed in the present report. Fracture spacing is also discussed in the present report but is less reliable because most borehole flowmeter surveys are from wells with a short open interval. Nevertheless, this estimate of fracture spacing is more reliable than are fracture counts in cores and on outcrops because many fractures have minimal flows of water. Water table fluctuations were measured at monitoring wells, but only a few well records are available for the Knox aquifer. Specific yield, maximum discharge, and average discharge were determined by hydrograph analysis for Ish Creek and the headwaters of Melton Branch. Storage capacity was calculated from specific yield and the average water table fluctuation. The average transmissivity of low-permeability intervals was determined from a few slug tests. The hydraulic conductivities of low-permeability intervals, relatively permeable intervals, and the continuum were calculated from the average transmissivity and thickness of each unit. Hydraulic gradient was measured on water table maps. Average recharge was calculated from average discharge. Recharge may be much larger than average in fill areas, however, and may be smaller than average in urbanized areas.

**Table 1. Summary of hydrogeologic properties (average value or range)**

<b>Stormflow zone</b>		
Thickness		
Grassland (m)		0.2-0.4
Forest (m)		0.6-2.0
Infiltration rate		
Grassland (m/d)		1.1
Forest (m/d)		8.8
Total porosity		0.4
Macropore (>0.2 mm) porosity		$2 \times 10^{-3}$
Specific yield		0.035
Storage capacity ( $m^3/km^2$ )		$2.2 \times 10^4$
Hydraulic conductivity (m/d)		9.2
Hydraulic gradient		0.075
Discharge rate ( $L s^{-1} km^{-2}$ )		0-110
<b>Groundwater zone</b>	<b>Knox aquifer</b>	<b>ORR aquitards</b>
Thickness		
Relatively permeable interval (m)		1.5
Low-permeability interval (m)		12
Water table fluctuation (m)	5.3	1.5
Total porosity (matrix)		$9.6 \times 10^{-3}$
Fracture porosity		$5.0 \times 10^{-4}$
Specific yield	$3.3 \times 10^{-3}$	$2.3 \times 10^{-3}$
Storage capacity <sup>a</sup> ( $m^3/km^2$ )	$1.8 \times 10^4$	$3.4 \times 10^3$
Fractures		
Spacing (cm)		35
Aperture (mm)	0.25	0.12

Table 1 (continued)

Groundwater zone	Knox aquifer	ORR aquitards
Unfractured rock matrix		
Hydraulic conductivity (m/d)		8.7x10 <sup>-8</sup>
Low-permeability intervals		
Transmissivity (m <sup>2</sup> /d)		1.1x10 <sup>-3</sup>
Hydraulic conductivity (m/d)		4.0x10 <sup>-4</sup>
Relatively permeable intervals		
Transmissivity (m <sup>2</sup> /d)	1.0	0.12
Hydraulic conductivity (m/d)		0.068
Continuum		
Transmissivity (m <sup>2</sup> /d)	7.3	0.75
Hydraulic conductivity <sup>b</sup> (m/d)		0.18
Hydraulic gradient	0.02	0.05
Average recharge (mm)	65	20
Maximum discharge (L min <sup>-1</sup> km <sup>-2</sup> )	1030	280
Average discharge (L min <sup>-1</sup> km <sup>-2</sup> )	120	38

<sup>a</sup>Between high and low water table elevations.

<sup>b</sup>Relatively permeable intervals.

## 5. CHEMICAL CHARACTERISTICS OF GROUNDWATER

Groundwater in the water table and intermediate intervals of the groundwater zone in the ORR aquitards is a slightly acidic to moderately alkaline, calcium bicarbonate type. Magnesium and sodium typically occur in smaller and approximately equal amounts. Potassium, chloride, nitrate (as nitrogen), and sulfate generally have concentrations of only 1-15 mg/L. Sulfate contents of 30-300 mg/L occur in a few wells in the Conasauga Group and are apparently caused by the solution of gypsum. Most fluoride contents are <1.0 mg/L, but a few deeper wells in limestone units have natural fluoride contents of 2-12 mg/L. The larger fluoride concentrations are probably complexed with aluminum in water with a pH of >8.5. Iron and manganese contents rarely exceed secondary drinking water standards (0.3 and 0.05 mg/L) in filtered water samples, but most unfiltered samples exceed these standards. Relatively large concentrations (>0.1 mg/L) of other metals are common in groundwater from shale units and may occur with high concentrations of manganese in unfiltered water samples. Total dissolved solids are nearly always <500 mg/L.

Shallow groundwater in the Knox aquifer is a calcium-magnesium bicarbonate type; the Ca/Mg ratio values are typically in the range 1.0-2.5. Sodium concentrations are almost always <15 mg/L and are commonly 0.5-5 mg/L. The pH and the concentrations of other constituents in the Knox aquifer, including total dissolved solids, are about the same to somewhat lower than in groundwater from the ORR aquitards. However, the complex lateral flow paths for groundwater and the different contributions of upward and downward seepage to these flow paths in both the Knox aquifer and the ORR aquitards result in a large range in the concentrations of chemical constituents at shallow levels, both temporally and spatially.

A slightly alkaline to alkaline, sodium bicarbonate water type occurs in the deep interval of the groundwater zone. Water from some wells near the top of this zone has nearly equal amounts of calcium, magnesium, and sodium (Webster and Bradley 1987, pp. 91-93), but sodium concentrations at deeper levels may constitute >90% of all cations. Total dissolved solids increase with depth but are generally <500 mg/L near the top of the zone. This water type probably indicates sluggish groundwater flow. Corrected (for processes other than matrix diffusion) carbon-14 ages of water from seven wells in Melton Valley are 10,000-25,000 years. However, the samples contain 1-5 or more tritium units; the only natural source of tritium is the atmosphere; and tritium has a short half life (12.3 years). The presence of both new tritium and old carbon-14 indicates a mixture of young fracture water and old water from the rock matrix. Water samples from three wells 145-162 m deep in Bear Creek Valley showed an alkaline sodium chloride-bicarbonate water type with a pH in the range 8.5-10.0. This water probably represents a transition from a sodium bicarbonate type to a sodium chloride type and may occur near the base of groundwater circulation.

A nonpotable water with a dissolved solids content of 2,500-275,000 mg/L occurs below depths of 180 m in Melton Valley. This water is an acidic, sodium chloride type with lesser amounts of calcium and magnesium, minor amounts of strontium and bromide, and trace amounts of potassium, barium, lithium, manganese, and iron (Switek et al. 1987, p. 7; Haase et al. 1987, pp. 16-21). These characteristics are those of membrane-concentrated water (membrane-filtration theory; Freeze and Cherry 1979, pp. 292-295) and connate brine.

## 5.1 SPATIAL AND TEMPORAL VARIABILITY OF WATER CHEMISTRY

In upland areas of the ORR, the chemical characteristics of shallow groundwater are determined mostly by the local solubility of the rocks and by amounts of dilution during recharge events. Concentrations at any time may be nearly the same in small areas, but larger differences occur in larger areas. The average specific conductance of water in 12 wells at the small Environmental Test Facility (ETF) in WAG 6 near ORNL, for example, has a range of only 123-178  $\mu\text{mhos/cm}$  (Davis et al. 1984, pp. 159-170), but the range in average specific conductance for 14 other wells in WAG 6 is 270-1130  $\mu\text{mhos/cm}$ . Temporally, large changes in chemical concentrations occur for shallow wells in upland areas of the ORR aquitards, but only minor changes occur in deeper wells. Wells at the ETF site, for example, had ranges in specific conductance of 118-255  $\mu\text{mhos/cm}$  to 3-300  $\mu\text{mhos/cm}$ . Other data from the WAG 6 area show relatively large monthly changes in specific conductance of water and large ranges for wells <20 m deep but nearly constant values in deeper wells (Table 2).

In lowland areas near discharge locations, concentrations of chemical constituents are determined mostly by the nearly unique conditions along each of the groundwater flow paths that lead to these areas. As a result, the concentrations of the constituents are spatially more variable than for wells of the same depths in upland areas. Two sections near Whiteoak Creek, for example, show no apparent relationships between the specific conductance of water and the locations and depths of the screened intervals in these closely spaced wells (Fig. 10). On the other hand, monthly measurements of specific conductance have less temporal variability than do wells of the same depths in upland areas (Table 3). Some dilution by recharge water apparently occurs in lowland areas because the shallower well in each pair has a larger temporal variability than does the deeper well.

**TABLE 2. Temporal changes in the specific conductance of water for wells on hillslopes**

Well ID	644	645	646	641	638	652	651	656
Depth (m)	3.5	5.6	11	16	20	24	29	34
Date	Specific conductance ( $\mu\text{mhos/cm}$ )							
3-3-88	380	625	614	608	1061	300	332	600
4-8-88	321	674	599	546	1048	299	331	599
5-5-88	363	613	620	522	1012	299	333	600
6-9-88	332	675	579	478	920	283	314	550
6-29-88	203	743	620	531	1014	301	335	602
7-28-88	156	745	591	583	1019	300	330	597
8-31-88	349	756	626	830	1048	300	335	606
10-5-88	324	513	624	930	1020	301	334	609
11-1-88	338	525	734	879	1039	300	337	608
12-5-88	322	345	580	1022	1022	300	333	611
1-6-89	137			780	1013	301	333	605
2-15-89	326	698	578	521	971	301	335	609
3-9-89	278	716	543	497	946	301	335	609

**TABLE 3. Temporal changes in the specific conductance of water for wells near streams**

Well ID	774	775	776	777	778	779	784	785
Depth (m)	3.2	13	4.7	14	4.0	13	4.0	13
Date	Specific conductance ( $\mu\text{mhos/cm}$ )							
6-1-88	475	570	1024	673	623	570	704	452
6-29-88	428	574	1045	679	655	579	652	456
8-3-88	559	575	1060	675	648	580	719	378
8-31-88	443	571	1075	675	656	580	743	460
10-5-88	555	569	1077	668	652	577	740	439
11-1-88	563	578	1077	676	646	580	759	458
12-6-88	543	568	1096	661	635	578	691	455
1-6-89	366	565	1101	656	626	575	697	458
2-15-89	557	567	1022	657	644	581	677	468
3-9-89	396	565	987	655	648	581	667	464

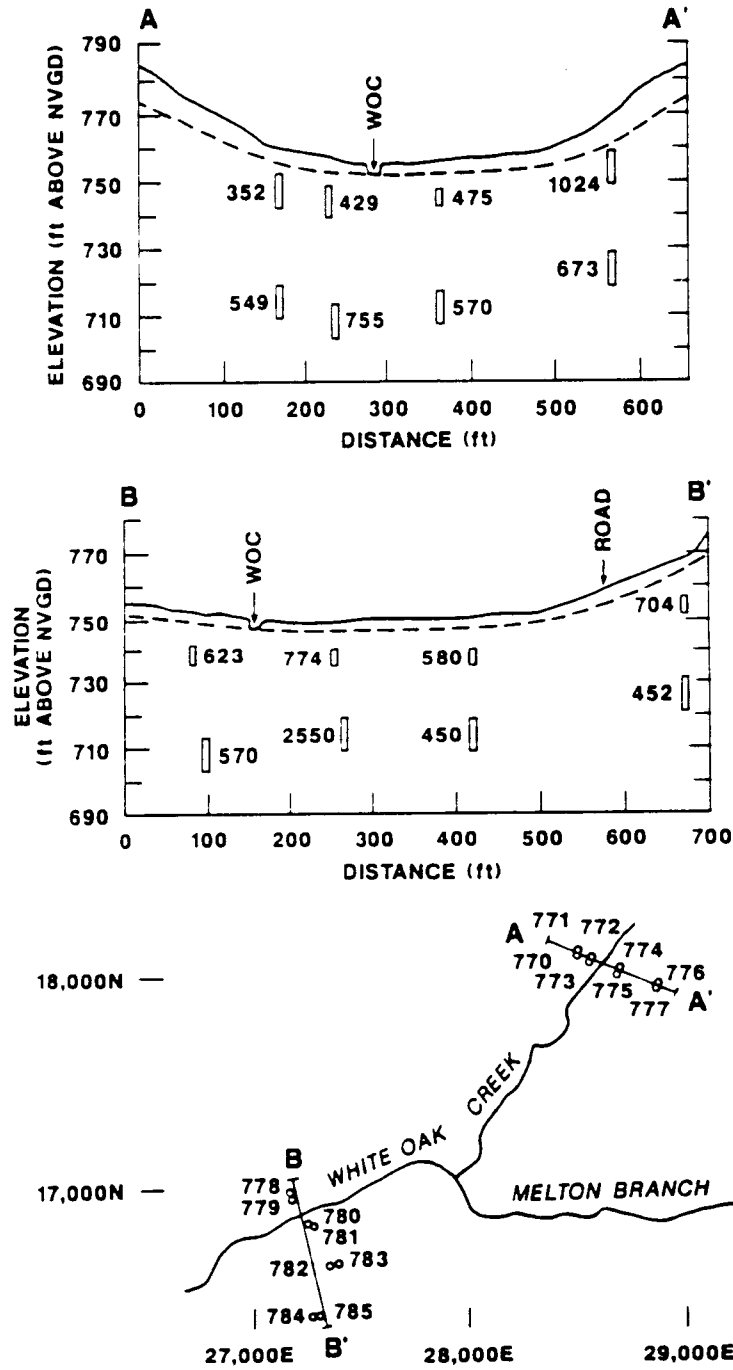


Fig. 10. Location map and sections showing specific conductance of water ( $\mu\text{mhos/cm}$ ) and screened intervals in paired shallow and deeper wells near the junction of Whiteoak Creek and Melton Branch.

The dilution effects of recharge occur mostly near the water table. For example, the standard deviations of monthly measurements of specific conductance (Fig. 11) from WAG 6 (hillslope locations) and WAG 2 (valley locations) near ORNL show an exponential decrease with depth. Each data point on Figure 11 was obtained by calculating the natural logarithm of the standard deviation of log-transformed monthly measurements of specific conductance; each data point represents 9-13 measurements over a period of 1 year. The lower position and steeper slope of the curve for wells in valley locations show that dilution effects are smaller and extend to shallower depths near discharge locations.

Because of the many flow paths and large differences in groundwater residence times, there is no apparent relationship between constituent concentrations and well depths up to depths of about 20-30 m in most areas of the ORR. Near the S-3 Ponds site at the Oak Ridge Y-12 Plant, however, the data below show that average contaminant concentrations in 1986-1989 were highest at depths of about 23 m. The lower concentrations in deeper wells are apparently caused by a smaller groundwater flux, and the lower concentrations in shallower wells apparently represent the results of natural flushing since the contaminant source was immobilized in 1983, as is discussed later.

Geometric mean concentration, 1986-89

Well depth (m)	No. wells	Nitrate nitrogen (mg/L)	Spec. cond. ( $\mu$ mhos/cm)	Dissolved solids (mg/L)
5-8	5	470	6060	3010
22-24	7	3010	20300	16000
43-46	2	405	3980	3130
165-175	2	3	2080	1300

## 5.2 EVIDENCE FOR GROUT CONTAMINATION

A few groundwater samples, which were obtained from newly constructed wells on the ORR, had a pH >9.5, and one possible explanation for the alkaline water is grout contamination. This type of contamination might result from a release of high pH water during emplacement and setting of the grout or from later leaching by groundwater flow through fractures in the grout and the

ORNL-DWG 92M-12362

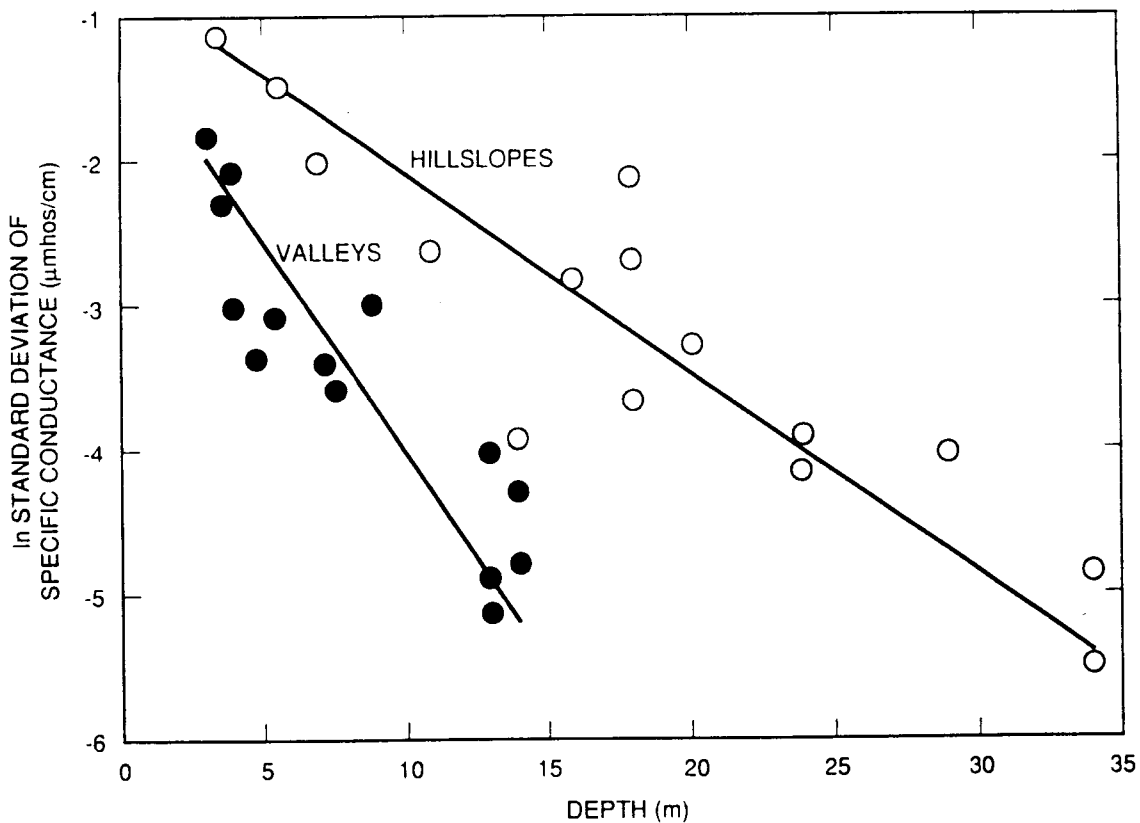


**Fig. 11. Relationship of the standard deviation of specific conductance to well depth.**

adjacent rocks. Water chemistry data from six wells (GW-143, GW-145, GW-146, GW-153, GW-159, and GW-220), which are completed in the Knox aquifer near the Oak Ridge Y-12 Plant, apparently show the effects of grout contamination. The pH of the first five water samples from each well in 1986-87 was 9.6-12.1 whereas the pH of later samples was 6.5-9.0, which is the normal range for shallow, uncontaminated groundwater.

The concentrations of most chemical constituents in the early groundwater samples are within the normal range (within one standard deviation of the geometric mean; Solomon et al. 1992, p. 3-32). Also, there are not the anomalously high concentrations of aluminum, fluoride, and silicon that would be expected in groundwater with a high pH. These results suggest that the high pH water is not in equilibrium with the minerals in the surrounding rocks.

The early water samples have potassium contents larger than the geometric mean plus one standard deviation (8.5 mg/L) for groundwater, and the potassium concentration is larger than that of sodium in nearly all of the samples, including samples in 1987-1989. In most natural groundwater, the Na/K ratio is 2-10 (Hem 1970, p. 151). Also, the aluminum and fluoride concentrations in both early and later water samples are a little higher than the normal range. Third, the concentration of calcium is only about 10-times larger than that of strontium whereas the Ca/Sr ratio in most limestones is >1000 (Hem 1970, p. 195). Finally, the concentrations of chloride and sulfate are near the upper end of the normal range in some of the early water samples.

Average potassium concentrations in the water samples are clearly associated with average pH, as shown in the data below.

	1986	1987	1988	1989
pH	10.2	8.4	8.0	7.7
Potassium (mg/L)	42	12	12	11

The likely source of both the alkaline water and the anomalous potassium content is the release of fluids from grout during emplacement and setting; the original source of potassium probably is the clay content of the cement. Nearly all decreases in pH and potassium content occurred within the first year, but the changes required at least three cycles of well purging and sampling. There was thus a significant cost associated with the removal of the contaminants. Also, the potassium content of most water samples from the six wells in 1989 was larger than that of sodium, and additional decreases in potassium may occur in the future.

The relatively large concentrations of aluminum, chloride, fluoride, strontium, and sulfate might be anomalous, but it is less likely that grout is the source of any contamination. Gypsum is a common source of sulfate in groundwater and is a common minor constituent of cement, sodium bentonite (which may have been used as a seal between the sandpack and the grout), and rocks on the ORR. Also, these constituents might be secondary contaminants that were produced by differential solution of rocks or grout exposed to alkaline water. Whatever the source, the concentration of strontium was 3.4-7.0 mg/L, and the concentration of sulfate was 30-45 mg/L in three wells after 4 years of purging and sampling. Thus, a determination as to whether or not the relatively large concentrations were produced by contamination during well construction might be important for a comparison of the results of upgradient versus downgradient monitoring.

### 5.3 EVIDENCE FOR CONTAMINANT FLUSHING BY NATURAL PROCESSES

Data from the S-3 Ponds site near the western edge of the Oak Ridge Y-12 Plant show a reduction through time in the concentrations of contaminants that are discharged to the headwaters of Bear Creek. This natural flushing is apparently occurring mostly near the water table, but the process is slowly reducing contaminant concentrations in both groundwater and surface water.

The four-pond cluster at the S-3 site was constructed in 1951; the ponds covered a total area of about 15,000 m<sup>2</sup> and were about 5 m deep. While in operation, the ponds received low-pH liquid wastes, including metals dissolved in nitric acid. The normal water level in the ponds was about 4 m above the water table, resulting in downward percolation of pollutants (Geraghty and Miller Inc. 1989a, p. 3-1). Disposals to the ponds were reduced in 1976 and ended in 1983. In preparation for later closure, water in the ponds was neutralized in June 1983 by adding limestone, quicklime, and sodium hydroxide until the pH was >9.0. This process caused precipitation of most dissolved cations and resulted in the accumulation of 0.6-1.5 m of sludge (Geraghty and Miller Inc. 1989a, p. 3-2). Biological denitrification of the water began in June 1983 and continued through September 1984. Beginning in 1988, the sludge was stabilized with coarse aggregate, a five-layer cap was used to fill and seal the ponds, and an asphalt parking lot was constructed over the site.

In 1986-1989, groundwater from wells near the contaminant plume of the S-3 Ponds site had nitrate concentrations, as nitrogen, from <1 mg/L to >25,000 mg/L. The proposed Alternative Concentration Limit (ACL; Geraghty and Miller Inc. 1989a, p. 8-6) for nitrogen is 900 mg/L, and this is the only groundwater constituent that exceeds the proposed limits for the contaminant plume. A cumulative probability graph of the arithmetic means of nitrogen concentrations in all samples from these wells shows two populations (Fig. 12), which are lognormally distributed. The population at the lower left on the graph consists of data from wells on the southern sides of Bear Creek and East Fork Poplar Creek. The lower concentrations of nitrogen in water from these wells apparently represents flow under the axis of the valley in the Maynardville Limestone (Knox aquifer) and dilutions by uncontaminated groundwater flows from Chestnut Ridge. The geometric mean of the nitrogen concentrations in this population is 18 mg/L.

The population on the upper right of the graph represents concentrations of nitrogen at both shallow and deeper levels along the main groundwater flow paths from the S-3 site. The geometric mean of the nitrogen concentrations is 1300 mg/L, and the range from the mean minus one to the mean plus one standard deviation is 220-7300 mg/L.

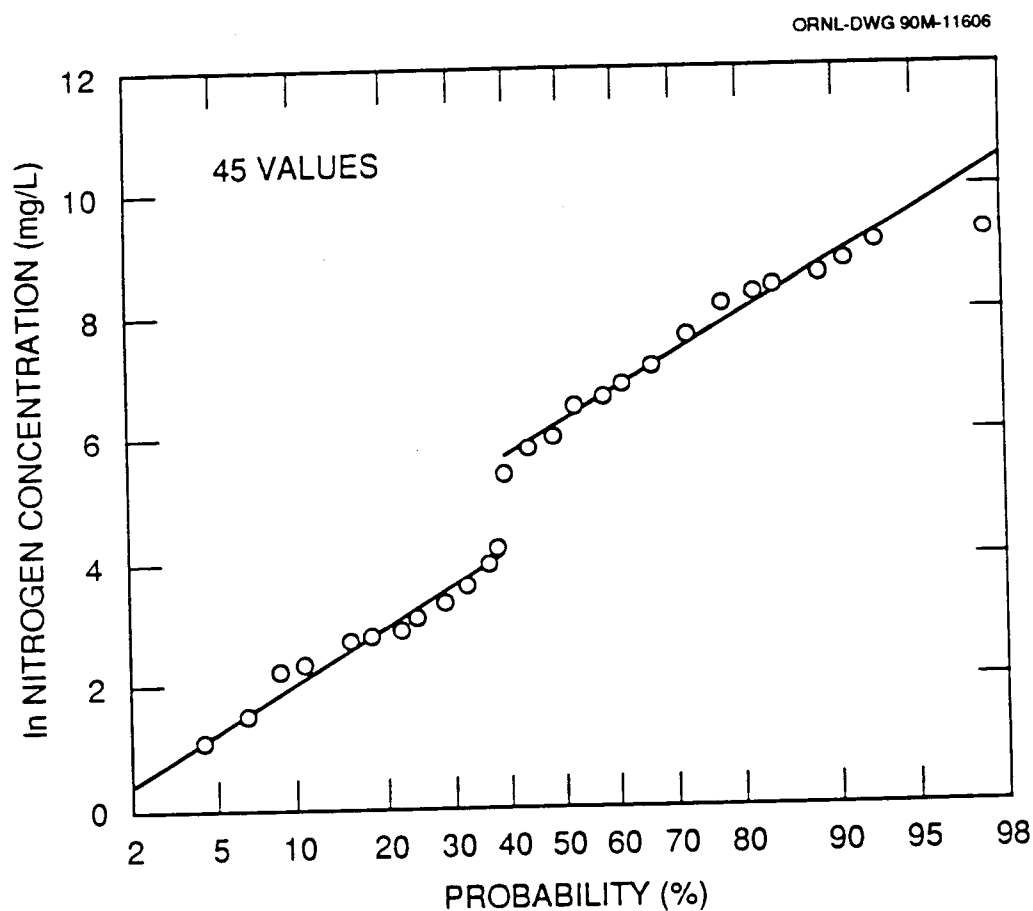


**Fig. 12. Cumulative probability graph of nitrate concentrations, as nitrogen, in groundwater near the site of the S-3 Ponds, 1986-1989.**

Three monitoring wells (GW-106, GW-127, and GW-276) near the water table in the area of the contaminant plume at the S-3 Ponds site show an exponential decrease in concentrations of nitrate as nitrogen beginning in mid-1987 (Fig. 13). The reasons why this trend does not occur earlier and why similar trends have not been detected for other monitoring wells may be related mostly to the purging procedure before sampling. Pumping pulls water from nearby, less permeable fractures where water may be nearly stagnant between sampling events. Although contaminants probably diffuse into all fractures from the rock matrix, the contaminants are diluted and transported toward discharge locations in the more pervious fractures. In less pervious fractures, concentrations may increase because the rate of molecular diffusion exceeds the rate of groundwater flow. If this hypothesis is correct, in situ monitoring with a nitrate-specific probe or sampling without purging would show exponentially decreasing concentrations in nearly all monitoring wells. The hypothesis is likely because of the exponentially decreasing concentrations of contaminants in groundwater discharge to Bear Creek, as discussed below, and because the average concentration of nitrogen is lower near the water table, where flushing should have been most effective, than at somewhat deeper levels.

Groundwater from the site of the S-3 Ponds is discharged into the headwaters of Bear Creek and, probably, into the storm drain system at the Y-12 Plant. Data from station 12.46 (20.05 km above the mouth) on Bear Creek show that neutralization of water in the S-3 Ponds in June 1983 affected the chemical concentrations of groundwater discharge in September (Table 4). Neutralization had the effect of removing the source of groundwater contamination, and all later data show the slow flushing of primary pollutants (constituents in the disposals) and secondary pollutants (constituents that were dissolved by acid waters) from the rocks. The large early decrease in the concentrations of many constituents is

important because similar results might be obtained by hydrologic isolation of burial trenches and other solid waste management units on the ORR.

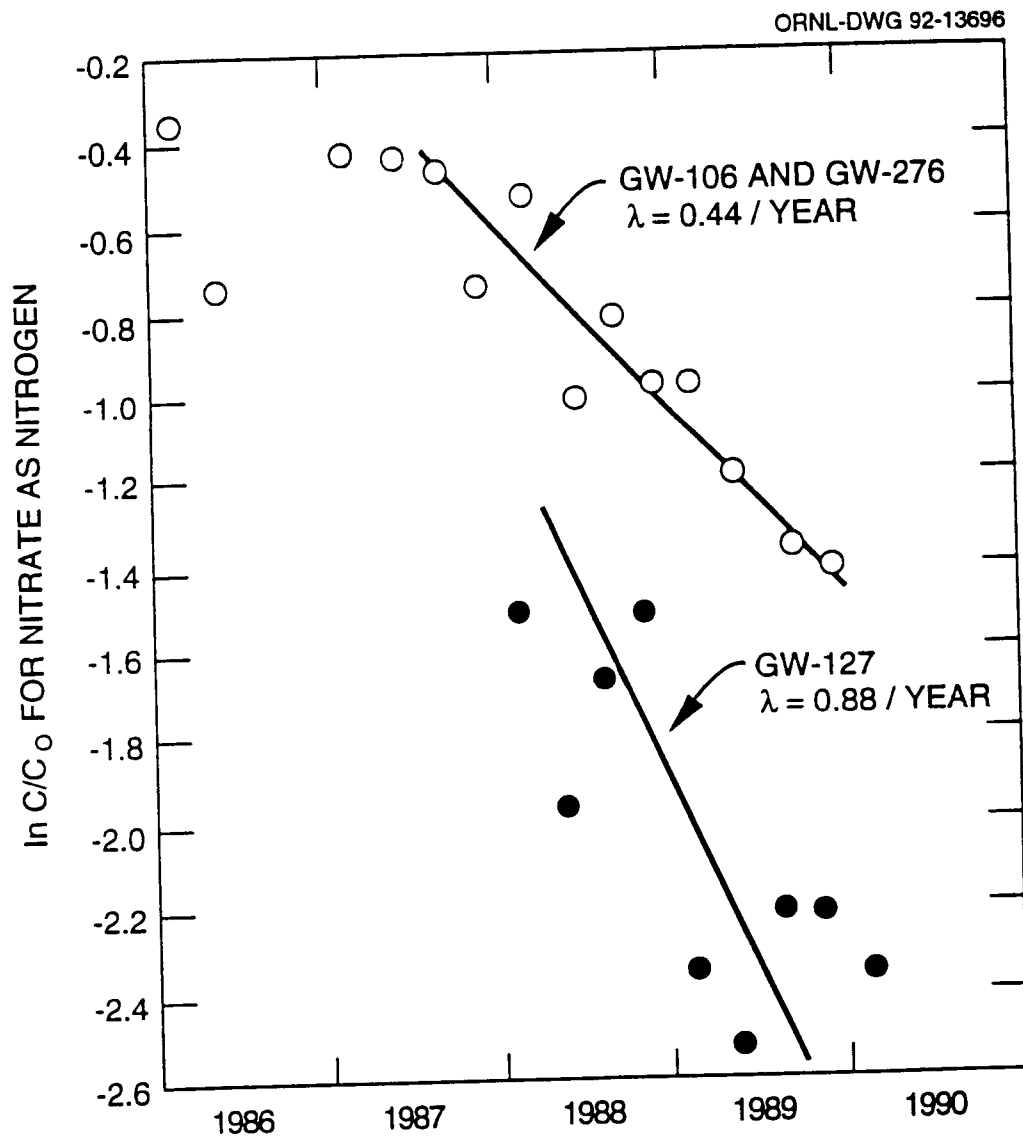


Fig. 13. Average normalized concentrations of nitrate as nitrogen in wells GW-106, GW-127, and GW-276.

**Table 4. Concentrations of major constituents in water from station 12.46 on Bear Creek during part of 1983.**

Concentrations (mg/L)												
1983	pH	TDS <sup>a</sup>	Al	Ca	F	K	Mg	Mn	Na	N <sup>b</sup>	Sr	U
7-28	4.0	10000	190	1300	39	35	170	27		1600	1.9	21
8-5	4.1	9400	190	920	40	33	170	31	380	1500	1.8	19
8-16	4.3	8000	66	870	21	26	140	20	260	1500	1.6	8.5
8-25	4.2	9300		1100	28	38	200	24	370	1800	2.1	11
8-31	4.3	8800	110	740	28	44	190	36	400	1400	2.7	
9-7	4.4		100	1300	26	40	200	37	330	1400	2.4	12
9-14	4.5	5500	64	660	17	28	130	16	210		1.7	8.8
9-21	4.5	6500	110	620	17	24	110	14	210	1100	1.4	8.6
-----												
9-29	6.5	3100	3.6	550	4.2	15	78	4.6	130	400	1.2	0.9
10-5	6.1	4400	4.6	550	3.1	17	58	7.1	98	1900	1.2	0.7
10-26	6.7	2220	3.1	390	0.8	10	48	3.1	70	210	0.7	1.0
10-31	6.2	2800	4.2	440	1.6	11	65	4.6	98	300	0.9	1.0
11-21	6.7	1400	2.5	220	2.2	6.5	25	1.9	39	180	0.5	0.4
12-5	6.1	1400	6.1	270	4.2	8.4	29	3.1	59	240	0.5	0.4
12-13	6.3	1600	4.6	240	3.7	8.1	26	2.9	64	970	0.5	0.3
12-19	7.1	2100	2.8	380	3.9	9.2	60	2.7	70	1200	0.8	1.1

<sup>a</sup>Total dissolved solids. <sup>b</sup>Nitrate as nitrogen.

Water samples were collected from Bear Creek at stations 12.46 (1983-87) and 11.97 (1989-91) on a weekly schedule without regard to precipitation events or flow conditions. Many of the water analyses represent dilution by recharge events and, probably, some contributions of overland runoff and subsurface stormflow to groundwater discharge. Also, the concentrations of all constituents in the water samples were variable, and there are no apparent correlations between the weekly and monthly concentrations. Nevertheless, a visual inspection of the data indicates a general trend of decreasing concentrations with time.

To predict the future concentrations of contaminants in Bear Creek, the data for the major constituents were selected, averaged, and normalized. First, an assumption was made that the highest weekly concentration of each constituent each month represents pure groundwater discharge. The resulting monthly concentration data were totaled, and an average annual concentration was calculated for each constituent. These annual concentrations were then plotted on a graph of log concentration versus time. The graphs are irregular, but eight constituents (calcium, magnesium, manganese, nitrate as nitrogen, potassium, sodium, strontium, and total dissolved solids) plot in a narrow band that seems to have a single characteristic slope. A second group of constituents (aluminum, fluoride, and uranium) plots in a different position on the graph and has a steeper slope. The steeper slope may occur because the concentrations of these constituents are pH dependent and because each constituent forms complexes with the others. Aluminum forms complexes with fluoride and silica in acid water (Hem 1970, p. 177), and uranium forms complexes with fluoride, phosphate, and bicarbonate at both low- and high-pH levels (Drever 1988, pp. 336-337).

Next, the concentration data for each group of constituents were normalized as  $C/C_0$ , where  $C$  is the average annual concentration after 1983, and  $C_0$  is the average 1983 concentration before water in the ponds was neutralized. The natural logarithm of the average normalized ratio value for each group was then plotted (Fig. 14). The slope of the straight line through the data points is a measure of the average change in concentration for each group of constituents:

$$\lambda = [\ln(C_1/C_0) - \ln(C_2/C_0)]/(\Delta t) , \quad (1)$$

$$C_2 = C_1/\exp(\lambda\Delta t) , \quad (2)$$

$$t_{0.5} = \ln(2)/\lambda , \quad (3)$$

where  $C_1$  is the concentration at time  $t_1$ ,  $C_2$  is the concentration

at time  $t_2$ ,  $C_0$  is the original concentration,  $\Delta t$  is  $t_2$  minus  $t_1$ ,  $\lambda$  is the slope of the graph in units of inverse time, and  $t_{0.5}$  is the half life of the contaminant. The slope is 0.16/year for the first group of constituents (including nitrate as nitrogen) and 0.36/year for the second group; the half life for the first group is 4.3 years, and the half life for the second group is 1.9 years.

The average future concentrations of the contaminants discharged into Bear Creek from the site of the S-3 Ponds can be calculated with eq. (2). These calculations show that all parameters except total dissolved solids and nitrate as nitrogen will drop to background levels (values less than one standard deviation above the geometric mean for groundwater; Solomon et al. 1992, p. 3-32) by 1995. The average content of total dissolved solids will drop below 500 mg/L (the recommended secondary limit for drinking water) by 2002. The average concentration of nitrogen will fall below the drinking water limit (10 mg/L) by 2012, and will drop to background levels (<3.9 mg/L) by 2022. These calculations assume, however, that the half life of the contaminants will not change in the future. Also, the results may not be applicable to other contaminants, such as organics.

The rate of decrease in contaminant concentrations near the S-3 Ponds site is determined by the relative proportions of groundwater storage and recharge. The dilution equation is

$$C_2 = C_1 q_1 / (q_1 + q_2) , \quad (3)$$

where  $q_1$  ( $L^3/L^2$ ) is the amount of groundwater storage at the time of the annual low water table, and  $q_2$  is annual recharge. Combining equations (2) and (3),

$$\begin{aligned} C_1 / \exp(\lambda t) &= C_1 q_1 / (q_1 + q_2) , \\ q_2 &= q_1 [\exp(\lambda t) - 1] . \end{aligned} \quad (4)$$

For  $\lambda = 0.16/\text{year}$  and  $t = 1$  year,

$$q_2 = 0.17 q_1 . \quad (5)$$

Equation (5) indicates that groundwater storage in this area is 5.8-times larger than average annual recharge.

The relative proportions of groundwater storage and annual recharge indicate that the rock matrix represents a reservoir for the slow release of contaminants, by molecular diffusion, into the fracture flow system. If total porosity of the rocks is  $9.6 \times 10^{-3}$ , total storage to a depth of 15-30 m below the water table (the main zone of mixing) is about 14-29 cm of water, and annual recharge is about 2.4-4.9 cm of water. This result is reasonable

ORNL-DWG 92M-12360

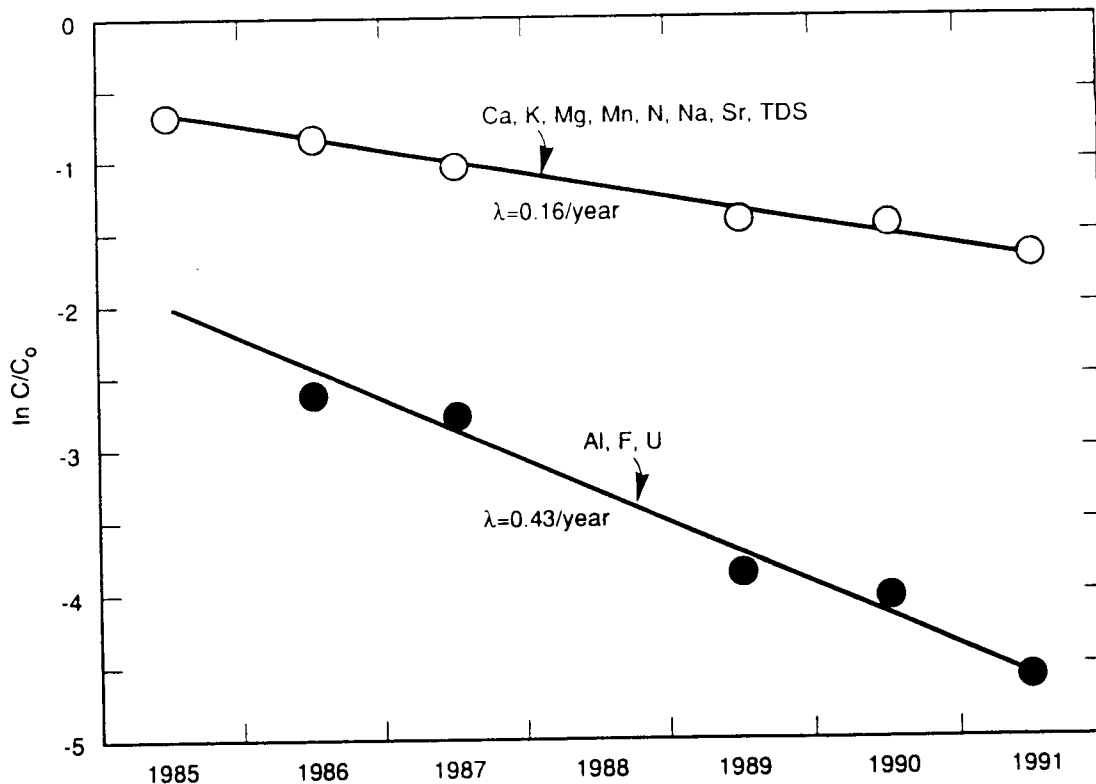


**Fig. 14. Graph of average normalized concentrations for the major constituents in Bear Creek.**

because other data show that average annual recharge on the ORR is about 2.0-6.5 cm of water (Solomon et al. 1992, p. 3-16). If all contaminants were stored in pervious fractures, however, average specific yield is  $7.6 \times 10^{-4}$ , and storage to a depth of 15-30 m below the water table is 1.1-2.3 cm of water. For these conditions, average annual recharge would be only 2-4 mm of water, and this result is unreasonable.

If the rate of contaminant release from the rock matrix into the fracture flow system is controlled by the rate of molecular diffusion, contaminant flushing by natural processes may prove to be nearly as effective as would remedial action by groundwater pumping. Pumping would have the initial effect of (1) removing contaminated water from the fracture flow system and pulling in uncontaminated or less contaminated water from nearby areas and (2) increasing the hydraulic gradient and the concentration gradient from the matrix into the fractures. Within an estimated period of 1-5 years, however, the hydraulic gradient would be near zero and the concentration gradient would decrease to a nearly constant value. Thereafter, pumping would be no more effective than would dilution and flushing by natural recharge and discharge.

## 6. SUMMARY OF GROUNDWATER MODELING

A variety of numeric models have been used to simulate groundwater flow and contaminant transport on the ORR. One-dimensional, lumped-parameter models or analytic solutions have been commonly used for calculations of the average flow and transport flux. These simple models, however, cannot adequately describe the spatial differences and temporal variations in the three-dimensional flow fields, and they are not discussed further in this report. Most of the modeling has used two-dimensional, steady-state, porous-media codes. Although these models provide limited information on a system that has three-dimensional flows in pervious fractures, flows in the deep interval and in the lower part of the intermediate interval of the groundwater zone can be adequately described for most purposes by a porous-media model. Codes developed by the U.S. Geological Survey (USGS), such as MODFLOW and MOC, and ORNL codes, such as FEMWATER and FEMWASTE, have been the most commonly used.

Several models have been developed for Bear Creek Valley and Melton Valley. Tucci (1986) and, more recently H. H. Zehner and P. Tucci (USGS, personal communication, 1991) constructed cross-section and limited three-dimensional models in Melton Valley. Bailey and Lee (1991) and Bailey (1988) of the USGS described the results of a cross-section model and a three-dimensional MODFLOW model of Bear Creek Valley. This MODFLOW model cannot be considered fully three-dimensional, however, because of the coarseness of the grid in the vertical direction and the limited data for vertical calibration. Using a similar approach, Geraghty and Miller, Inc. (1989b) set up a MODFLOW model of Bear Creek Valley. The boundary conditions and calculated potentiometric heads from this model were then used in a contaminant transport model, SWIFT, to simulate a small area around the plume from the site of the

S-3 Ponds (Geraghty and Miller, Inc. 1989c). However, the lack of transient data prevented exploration of remediation strategies.

Toran and Saunders (1992) recently constructed a two-dimensional cross-section model across Bear Creek Valley where more vertical data were available from multilevel monitoring wells, and found that geochemical data were important for the delineation of relatively permeable intervals. They also used a new particle tracking feature of MODFLOW to assess flow rates and directions.

The hydraulic conductivity values used in the large-area models (Table 5) were similar and conservative. The shallowest layer in each model was assigned a hydraulic conductivity in the range  $10^{-4}$  to  $10^{-6}$  cm/s, and the deepest layer was given a hydraulic conductivity in the range  $10^{-6}$  to  $10^{-9}$  cm/s. As described previously, the average hydraulic conductivity of the permeable intervals is about  $10^{-3}$  to  $10^{-4}$  cm/s; the average hydraulic conductivity of an equivalent porous medium at shallow depths would be about  $10^{-4}$  to  $10^{-5}$  cm/s. As also described previously, the average hydraulic conductivity of the relatively impermeable intervals is about  $5 \times 10^{-7}$  cm/s.

Less reliable hydraulic conductivity values were assigned to geologic units in the large-area models. There is no evidence that local differences in the hydraulic conductivity of geologic units in either the Knox aquifer or the ORR aquitards are applicable to larger areas. Also, the hydraulic conductivity data were not tested to determine whether or not the differences were statistically significant. The large-area models do show potentiometric-head and velocity differences that are typical of those produced by local differences in hydraulic conductivity, but these differences are not necessarily representative of the labeled geologic units.

**Table 5. Comparison of selected numerical models for groundwater flow on the Oak Ridge Reservation.**

No.	Model type and location	Source or reference	Layer base (m)	Hydraulic conductivity (cm/s)	Recharge (mm/yr)
1	Limited three-dimensional; Bear Cr. Valley	Bailey and Lee (1991)	15 30 122 183	$6 \times 10^{-6}$ to $1 \times 10^{-4}$ $6 \times 10^{-6}$ to $1 \times 10^{-4}$ $6 \times 10^{-6}$ to $1 \times 10^{-4}$ $3 \times 10^{-7}$	102-127 Ridges only
2	Cross section; Bear Cr. Valley	Toran and Saunders (1992)	46 260 381	$5 \times 10^{-5}$ $9 \times 10^{-6}$ $3 \times 10^{-8}$	25.4
3	Limited three-dimensional; Bear Cr. Valley	Geraghty and Miller (1989b)	30 61 122	$2 \times 10^{-5}$ to $7 \times 10^{-4}$ $1 \times 10^{-5}$ to $3 \times 10^{-4}$ $5 \times 10^{-6}$ to $2 \times 10^{-4}$	305
4	Limited three-dimensional; S-3 Ponds site	Geraghty and Miller (1989c)	9 18 30 61 122	$1 \times 10^{-5}$ to $6 \times 10^{-4}$ $2 \times 10^{-5}$ to $8 \times 10^{-4}$ $2 \times 10^{-5}$ to $7 \times 10^{-4}$ $8 \times 10^{-6}$ to $3 \times 10^{-4}$ $4 \times 10^{-6}$ to $2 \times 10^{-4}$	305
5	Cross section; Melton Valley	H. H. Zehner and P. Tucci, USGS	15 30 76 381	$1 \times 10^{-5}$ to $1 \times 10^{-4}$ $1 \times 10^{-6}$ to $1 \times 10^{-4}$ $4 \times 10^{-7}$ to $4 \times 10^{-6}$ $4 \times 10^{-9}$	102-127 Ridges only
6	Limited three-dimensional; Melton Valley	H. H. Zehner and P. Tucci, USGS	15 30 76 183	$7 \times 10^{-5}$ $2 \times 10^{-5}$ $4 \times 10^{-6}$ $4 \times 10^{-9}$	102-127 Hills and ridges only

Table 5 (continued)

Layer No.	base (m)	-----Hydraulic conductivity (cm/s)-----						
		Cr	Cpv	Crt & Crg	Cm	Cn	Cmn	Ock
1	15	1.1x10 <sup>-4</sup>	5.6x10 <sup>-6</sup>	1.3x10 <sup>-5</sup>	1.2x10 <sup>-5</sup>	2.1x10 <sup>-5</sup>	1.4x10 <sup>-5</sup>	1.1x10 <sup>-5</sup>
	30	1.1x10 <sup>-4</sup>	5.6x10 <sup>-6</sup>	1.3x10 <sup>-5</sup>	1.2x10 <sup>-5</sup>	2.1x10 <sup>-5</sup>	1.4x10 <sup>-5</sup>	1.1x10 <sup>-5</sup>
	122	1.1x10 <sup>-5</sup>	5.6x10 <sup>-7</sup>	1.3x10 <sup>-6</sup>	1.2x10 <sup>-6</sup>	2.1x10 <sup>-6</sup>	1.4x10 <sup>-6</sup>	1.1x10 <sup>-6</sup>
	183	2.8x10 <sup>-7</sup>	2.8x10 <sup>-7</sup>	2.8x10 <sup>-7</sup>	2.8x10 <sup>-7</sup>	2.8x10 <sup>-7</sup>	2.8x10 <sup>-7</sup>	2.8x10 <sup>-7</sup>
2	46	4.6x10 <sup>-5</sup>	4.6x10 <sup>-5</sup>	4.6x10 <sup>-5</sup>	4.6x10 <sup>-5</sup>	4.6x10 <sup>-5</sup>	4.6x10 <sup>-5</sup>	4.6x10 <sup>-5</sup>
	260	1.1x10 <sup>-5</sup>	3.0x10 <sup>-7</sup>	3.0x10 <sup>-6</sup>	3.5x10 <sup>-7</sup>	4.7x10 <sup>-7</sup>	7.5x10 <sup>-6</sup>	4.1x10 <sup>-5</sup>
	381	3.0x10 <sup>-8</sup>	3.0x10 <sup>-8</sup>	3.0x10 <sup>-8</sup>	3.0x10 <sup>-8</sup>	3.0x10 <sup>-8</sup>	3.0x10 <sup>-8</sup>	3.0x10 <sup>-8</sup>
3	30		3.9x10 <sup>-5</sup>	3.9x10 <sup>-5</sup>	1.7x10 <sup>-4</sup>	3.0x10 <sup>-4</sup>	7.0x10 <sup>-4</sup>	1.9x10 <sup>-5</sup>
	61		2.0x10 <sup>-5</sup>	2.0x10 <sup>-5</sup>	8.7x10 <sup>-5</sup>	1.5x10 <sup>-4</sup>	3.5x10 <sup>-4</sup>	9.6x10 <sup>-6</sup>
	122		9.8x10 <sup>-6</sup>	9.8x10 <sup>-6</sup>	4.4x10 <sup>-5</sup>	7.6x10 <sup>-5</sup>	1.7x10 <sup>-4</sup>	4.8x10 <sup>-6</sup>
4	9		3.1x10 <sup>-5</sup>	3.1x10 <sup>-5</sup>	1.2x10 <sup>-4</sup>	2.7x10 <sup>-4</sup>	6.2x10 <sup>-4</sup>	1.5x10 <sup>-5</sup>
	18		3.9x10 <sup>-5</sup>	3.9x10 <sup>-5</sup>	1.5x10 <sup>-4</sup>	3.4x10 <sup>-4</sup>	7.0x10 <sup>-4</sup>	1.8x10 <sup>-5</sup>
	30		3.5x10 <sup>-5</sup>	3.5x10 <sup>-5</sup>	1.3x10 <sup>-4</sup>	3.0x10 <sup>-4</sup>	7.0x10 <sup>-4</sup>	1.7x10 <sup>-5</sup>
	61		1.7x10 <sup>-5</sup>	1.7x10 <sup>-5</sup>	6.5x10 <sup>-5</sup>	1.5x10 <sup>-4</sup>	3.5x10 <sup>-4</sup>	8.3x10 <sup>-6</sup>
	122		8.7x10 <sup>-6</sup>	8.7x10 <sup>-6</sup>	3.3x10 <sup>-5</sup>	7.6x10 <sup>-5</sup>	1.7x10 <sup>-4</sup>	4.2x10 <sup>-6</sup>
5	15		8.8x10 <sup>-6</sup>	9.9x10 <sup>-5</sup>	6.0x10 <sup>-5</sup>	1.1x10 <sup>-4</sup>	1.4x10 <sup>-5</sup>	
	30		3.5x10 <sup>-6</sup>	1.2x10 <sup>-4</sup>	1.8x10 <sup>-5</sup>	4.9x10 <sup>-5</sup>	1.4x10 <sup>-6</sup>	
	76		3.5x10 <sup>-7</sup>	3.5x10 <sup>-7</sup>	1.1x10 <sup>-6</sup>	3.5x10 <sup>-6</sup>	3.5x10 <sup>-7</sup>	
	381		3.5x10 <sup>-9</sup>					
6	15		6.7x10 <sup>-5</sup>					
	30		1.8x10 <sup>-5</sup>					
	76		3.5x10 <sup>-6</sup>					
	381		3.5x10 <sup>-9</sup>					

Cr: Rome Formation; Cpv: Pumpkin Valley Shale; Crt: Rutledge Limestone;  
 Cm: Maryville Limestone; Cn: Nolichucky Shale; Cmn: Maynardville Limestone;  
 Ock: Knox Group.

Other misrepresentations of the hydrogeologic system in one or more of the older large-area models include the omission of a high-permeability, near-surface stormflow zone, the input of as much as 100-300 mm/year of recharge to the water table, the calibration result that recharge occurs only on hills and ridgetops, and the assumption of a temporally constant transmissivity (an unchanging saturated thickness). Because of these problems, the older models do not adequately represent subsurface flows at shallow depths. Nevertheless, the model results may approximate the flow and boundary conditions at deeper levels in the groundwater zone and may provide initial estimates for the parameter values and the boundary conditions in more detailed, local models.

The results from the large-area models were fairly similar, and some of the conclusions were (1) most groundwater flow (>90%) takes place in the upper 30 m below the water table; (2) the possibility of flow beneath ridges or streams cannot be evaluated because of lack of data for model calibration (with the exception of Toran and Saunders 1992), although it is unlikely that such flows occur in the shallow, active groundwater zone; (3) the vadose zone and the water table interval of the groundwater zone were not modeled because of grid and data limitations; and (4) the deep interval of the groundwater zone is recharged only on ridge tops. Specific suggestions in the reports included the need to determine the groundwater contribution to streamflow, the need for more reliable aquifer-test data, and the need for boundary-condition data.

A few detailed modeling efforts have been conducted in waste areas. These models have emphasized an understanding of the flow system rather than plume mapping, and none of the models is appropriate for predictions of future concentrations. Solomon and Yeh (1987) used the only true three-dimensional model (FEMWATER) on the reservation to model a single waste trench, which was

discretized with over 4500 nodes, and to determine whether water is perched or mounded in waste trenches above the water table. Separately, a two-dimensional flow model was constructed of the WAG-6 area near ORNL (Craig 1987), and it reproduced general head trends and the baseflow in tributary streams. The model was calibrated to a strike/dip anisotropy ratio of 2:1; no estimates of remediation effects could be conducted because of lack of transient data and boundary information. This effort was then extended to a transport model (starting with a new code and using MOC for transport) in order to predict transport times and contaminant concentrations in the streams for up to 500 years in the future (R. J. Luxmoore and J. M. Bowns, Oak Ridge National Laboratory, personal communication, 1992). The source terms were estimated with the UTM model. Because there were no distinct plumes for calibration, key parameters such as dispersion, porosity, and retardation could not be based on field data, and the results of this modeling effort are somewhat tentative. Another, smaller area in the east corner of WAG 6 has also been modeled (MODFLOW; O.R. West, Oak Ridge National Laboratory, Environmental Sciences Division, personal communication, Sept. 1991), but again, transient runs were not feasible.

Probably the first fracture flow model on the reservation was a simple one-dimensional parallel plate model along a cross section in Melton Valley (Toran et al. 1991). This model was used to explain old carbon-14 and young tritium in several wells about 60 m deep. The model showed that some tritium could travel rapidly along a fracture flow path and thus occur in the leading edge of a plume, but that most of the modern carbon-14 diffuses from fractures into the matrix and reaches a steady-state concentration. The same model has been used to explain tritium distributions in shallow cores in WAG 5 near ORNL and to predict how contamination diffuses from the rock matrix long after it would have been flushed from the fractures (Wickliff et al. 1991).

Current efforts focus on more complex processes and models. A true three-dimensional model in Melton Valley is being constructed to examine anisotropy ratios and to predict fluxes to streams from different components of the groundwater system. This effort takes advantage of ORNL's new supercomputer (Toran et al. 1992). A multiporosity scale model has also been constructed to reproduce transient storm events in Melton Branch Watershed (Gwo et al. 1991). A model calibrated with a tracer test using rhodamine dye in West Bear Creek Valley (Lee et al. 1989) is being reexamined in light of new hypotheses about fracture flow and matrix diffusion. Several general-purpose and site-based fracture flow models are also underway using new two-dimensional and three-dimensional codes developed at the University of Waterloo, Canada.

The goal of future efforts should be the incorporation of additional hydrologic detail or additional processes in the flow models. Flow systems in the stormflow zone and the water-table interval of the groundwater zone, for example, will probably require complex, three-dimensional, thin-layer, transient models in which transmissivity changes with saturated thickness during recharge and drainage events. Steady-state models are probably inappropriate in these intervals, where most subsurface flows occur. Integrated watershed analysis and water-budget modeling will also be needed to confirm the conceptual model of the shallow subsurface flow system.

Fractures are believed to be the key path for solute migration, but only porous media models have been applied to predict migration paths. Because of the uncertainty in fracture locations, sensitivity analysis, geostatistics, and hydrologic field data will be important in a successful program. One area of fracture flow modeling that is at the forefront of research is density-driven flows. A few unusually dense plumes (e.g. DNAPLs and high-concentration nitrate) occur on the ORR, and models can

be used to obtain an understanding of these systems; models for a preliminary analysis of these conditions have been acquired.

A well-balanced selection of numeric codes for groundwater modeling is presently available (Table 6), and the siting of one of DOE's supercomputing facilities at ORNL will facilitate the use of more detailed, more complex models. To successfully meet the groundwater-modeling goals required for waste-site closures, however, new data will be required for model calibration.

New and existing geochemical tracers of groundwater flow paths are needed in the future to integrate data at scales appropriate for predicting contaminant movement. Carbon-14 dating, tritium and helium analyses, and deuterium and oxygen-18 analyses are examples of geochemical tools that can provide key information on the dual porosity and dual permeability flow systems on the ORR. Similarly, more precise analyses of aluminum, silicon, and the ions in saline water are needed for adequate geochemical modeling and for predictions of flow-path lengths and travel times.

Future modeling efforts should take place in conjunction with field work, so that the model can be checked and calibrated or changed and updated, as new data come in. The goal is a flexible model that simulates the complex groundwater flow system.

Table 6. Index of Numerical Modeling Codes.

---

**Flow:**

FEMAIR, FEMWATER, FEWA, FLOWIADI, FLOWNET, MODFLOW, PFEM,  
VS2D

**Solute transport:**

AT123D, BIOPLUME II, CXTFIT, DISPER2, FEMA, FEMWASTE, MIGRAT,  
MOC, MT3D, Random Walk, SOFIT, SUTRA

**Coupled transport and geochemistry:**

HYDROGEOCHEM

**Fracture flow and transport:**

DPROTRAN, FRACTRAN, SWIFT/386, TRINET, TRAFRAP-WT

**Geochemical:**

MINEQL, PHREEQE (WATEQ), EQ3/6, HYDRAQL, SOLMINEQ, MINTEQ,  
GEOCHEM

**Geostatistical:**

AKRIP, COKRIG, Geo-EAS, GEOPACK, INVSOLN, SCOUT

**Stormflow/Recharge:**

HEC-1, HSPF, HELP, Wetting Front, UTM

**Pumping test and aquifer analysis:**

AQUISOLV, CLEARY AND PINDER WORKBOOK, PUMPTEST (IGWC), SLUGT,  
WALTON WORKBOOK, WHIP

---

## 7. CONCLUSIONS

Analysis and interpretation of recently acquired data corroborate the hydrogeologic model described by Solomon et al. (1992). All new data are from the groundwater zone, but in natural areas of the ORR, most subsurface water flows through the stormflow zone, which extends from land surface to a depth of 0.2-2 m. Thus, the stormflow and groundwater zones are interrelated components of the subsurface hydrologic system. In partly developed to urbanized areas of the ORR, the continuity of the stormflow zone is disrupted by impermeable barriers, drains, and permeable fills, including pipe-trench fill. Nevertheless, drain networks, fill materials, and remnants of the stormflow zone in these areas may link water source and water discharge areas.

There are five important principles for the occurrence and flow of groundwater on the ORR:

1. Average fracture permeability is 4-6 orders of magnitude larger than that of the rock matrix, but average fracture porosity is an order of magnitude smaller than that of the rock matrix. Pollutants are retarded by both sorption and matrix diffusion.
2. The groundwater flow system is recharge limited, and the total cross-sectional area of the pervious fractures transmits the average annual recharge to streams under the prevailing hydraulic gradient. Recharge rate also determines water table depth. Specific discharge and flux decrease with depth; groundwater below 50-100 m is old.
3. Subsurface flow occurs in thin layers. Flow is transient in the stormflow zone and variable in the water-table interval of the groundwater zone. Shallow flow paths are determined by the configurations of the stormflow zone and the water-table interval of the groundwater zone. At deeper levels, lateral flow paths are stratiform.

4. The properties of the continuum determine the groundwater flux. The average transmissivity of the continuum is larger than that near the average well.

5. Parameter values are lognormally distributed. Event recessions are first-order exponential curves.

Below the water table, the hydrogeologic framework consists of thin, relatively permeable fracture intervals, thicker, relatively impermeable fracture intervals, and a nearly impermeable rock matrix. Lateral flows of groundwater occur only in the permeable intervals. Fewer and less pervious fractures in the intervening rock layers connect the permeable intervals and produce continuity in the groundwater flow system. Groundwater flows are minimal in the rock matrix.

The average thickness of permeable intervals in wells is 1.5 m in areas of the ORR aquitards, and the range is about 0.25-7.5 m. These intervals consist of 1-3 pervious sections and intervening, less pervious sections. Each pervious section apparently consists of a single fracture that has a uniform hydraulic conductivity. About 40% of the pervious sections within 3.0 m of the water table have a thickness of >1.2 m, but at depths of >6.1 m below the water table, the average thickness of the pervious sections is 0.49 m, and none are >1.2 m thick. The average spacing of the pervious fractures is about 35 cm in the water-table and intermediate intervals of the groundwater zone.

The average hydraulic conductivity and aperture of pervious fractures in the ORR aquitards are nearly the same for fracture widths of <0.9 m, but decrease for wider fractures. This result shows a relationship between the cross-sectional area of the fracture opening and the maximum rate of groundwater flow; the width, aperture, and spacing of pervious fractures were probably formed by groundwater flows.

In the nonstratiform fracture network near the water table, most groundwater flows in the direction of the maximum hydraulic gradient. The remaining water follows fractures to deeper levels or lower elevations. Stratiform fractures in the intermediate interval of the groundwater zone transmit most water along strike toward cross-cutting, tributary streams. The remainder flows downdip, and then seeps upward through relatively impermeable rocks to discharge locations in main-valley streams. Very little groundwater flows through the deep interval because flow paths are longer, the hydraulic gradient is smaller, and the average permeability along the flow paths is much smaller.

In areas of the ORR aquitards, the average transmissivity of the continuum (0.65-0.75 m<sup>2</sup>/d) is 5 to 6 times larger than the geometric mean of transmissivity for the fractures that intercept wells (0.13 m<sup>2</sup>/d). This difference is probably caused mostly by the larger thickness of permeable intervals in a section of the continuum than in the open interval of the average well. However, the intersecting fracture network in the continuum may also transmit water in more directions than do the fractures that intercept the average well.

Water chemistry data show that recharge to the water table occurs nearly everywhere and periodically dilutes the concentrations of the chemical constituents in groundwater. These dilutions occur mostly near the water table, and temporal changes in water chemistry are larger for shallow wells than for deeper wells. The temporal changes are also larger for upland areas, where one component of the hydraulic gradient is downward, than for lowland areas, where the hydraulic gradient has an upward component. Spatially, the water chemistry is more variable in lowland than in upland areas because groundwater flow paths from all depths converge near discharge locations. Contaminant transport is retarded in part by matrix diffusion, and the rock

matrix may later act as a secondary source for contaminant releases to the fracture flow system.

Data near the site of the S-3 Ponds at the western edge of the Oak Ridge Y-12 Plant show a reduction through time in the concentrations of contaminants that are discharged to Bear Creek. Neutralization of water in the ponds in June, 1983 caused a large decrease in the concentrations of many contaminants in groundwater discharge during September of the same year. This change is important because similar results might be obtained by hydrologic isolation of other contaminant sources on the ORR. After data for 1985-91 have been averaged and normalized, the mean annual decrease in contaminant concentrations of the groundwater discharge to Bear Creek can be calculated and predicted. The results show that all contaminants, except total dissolved solids and nitrogen, will drop to background levels by 1995. Total dissolved solids will decrease to 500 mg/L by 2002; nitrogen will drop below the drinking water limit (10 mg/L) by 2012 and will decrease to background levels by 2022.

Numerical models of the subsurface flow system have not adequately described the thin-layer flows at shallow depths, but the model results may approximate groundwater flows and boundary conditions at deeper levels. The incorporation of additional detail for flows in the stormflow zone and the water-table interval of the groundwater zone will probably require three-dimensional, transient models in which saturated thickness and transmissivity change during recharge events and periods of water-level recession. Integrated watershed analysis and water-budget models are also needed to confirm the present concepts of the shallow subsurface flow systems. Finally, tracer tests and point-dilution tests are needed for evaluations of matrix diffusion processes and the changes in specific discharge with depth.

## 8. REFERENCES

- Bailey, Z. C., 1988. Preliminary evaluation of ground-water flow in Bear Creek Valley, the Oak Ridge Reservation, Tennessee. U.S. Geol. Survey Water Resources Investigations Report (WRIR) 88-4010, Nashville, Tenn.
- Bailey, Z. C., and R. W. Lee. 1991. Hydrogeology and geochemistry in Bear Creek and Union Valleys near Oak Ridge, Tennessee. U. S. Geol. Survey Water Resources Investigations Report (WRIR) 90-4008, Nashville, Tenn.
- Craig, P. M. 1987. Chapt. 8. Hydrogeologic modeling. In Summary of environmental characterization activities at the Oak Ridge National Laboratory Solid Waste Storage Area 6. Oak Ridge National Laboratory ORNL/RAP/LTR-87/68.
- Davis, E. C., W. J. Boegly, Jr., E. R. Rothschild, B. P. Spalding, N. D. Vaughan, C. S. Haase, D. D. Huff, S. Y. Lee, E. C. Walls, J. D. Newbold, and E. D. Smith. 1984. Site characterization techniques used at a low-level waste shallow land burial field demonstration facility. ORNL/TM-9146.
- de Laguna, W. T., T. Tamura, H. O. Weeren, E. G. Struxness, W. C. McClain, and R. C. Sexton. 1968. Engineering development of hydraulic fracturing as a method for permanent disposal of radioactive wastes. ORNL-4259.
- Diment, W. H., and E. C. Robertson. 1963. Temperature, thermal conductivity, and heat flow in a drilled hole near Oak Ridge, Tennessee. J. Geophy. Res. 68(17):5035-5047.
- Dreier, R. B., D. K. Solomon, and C. M. Beaudoin. 1987. Fracture characterization in the unsaturated zone of a shallow land burial facility. pp. 51-59. In Flow and Transport Through Fractured Rock. Am. Geophys. Union Monograph no. 42.
- Drever, J. I. 1988. The Geochemistry of Natural Waters, 2nd ed., Prentice Hall, Englewood Cliffs, N. J.

- Ford, D. C., and P. W. Williams. 1989. Karst Geomorphology and Hydrology. Unwin Hyman, London, United Kingdom.
- Freeze R. A., and J. A. Cherry. 1979. Groundwater. Prentice-Hall, Englewood Cliffs, N. J.
- Geraghty and Miller, Inc. 1989a. Alternate concentration limit demonstrations for the S-3 Waste Management Area, Y-12 Plant, Oak Ridge, Tennessee. Y/SUB89-00206C/11 for the Oak Ridge Y-12 Plant.
- Geraghty and Miller, Inc. 1989b. Development of ground-water flow models for the S-3 waste-management area Y-12 Plant, Oak Ridge, Tennessee. Y/SUB/89-00206C/1 for the Oak Ridge Y-12 Plant.
- Geraghty and Miller, Inc. 1989c. Development of contaminant transport models for four constituents at the S-3 waste-management area, Y-12 Plant, Oak Ridge, Tennessee. Y/SUB/89-00206C/3 for the Oak Ridge Y-12 Plant.
- Gwo, J. P., G. T. Yeh, G. V. Wilson, and P. M. Jardin. 1991. Modeling subsurface flow with a multi-region approach. Abstract. Am. Geophy. Union, EOS, 72:112.
- Haase, C. S., J. Switek, and S. H. Stow. 1987. Geochemistry of formation waters in the lower Conasauga group at the New Hydrofracture Facility: Preliminary data from the Deep Monitoring (DM) wells. ORNL/RAP-6.
- Haase, C. S., E. C. Walls, and C. D. Farmer. 1985. Stratigraphic and structural data for the Conasauga Group and the Rome Formation on the Copper Creek fault block near Oak Ridge, Tennessee: preliminary results from test borehole ORNL-Joy No. 2. ORNL/TM-9159.
- Hem, J. D. 1970. Study and interpretation of the chemical characteristics of natural water. U.S. Geol. Survey Water-Supply Paper 1473.
- Ketelle, R. H., and D. D. Huff. 1984. Site characterization of the West Chestnut Ridge site. ORNL/TM-9229.

- Lee, R. R., R. H. Ketelle, J. M. Bownds, and T. A. Rizk. 1989. Calibration of a groundwater flow and contaminant transport computer model - Progress toward model validation. ORNL/TM-11294
- McMaster, W. M. 1967. Hydrologic data for the Oak Ridge area, Tennessee. U.S. Geol. Survey Water-Supply Paper 1839-N.
- May, V. J., G. H. Wood, and D. R. Rima. 1970. A proposed streamflow-data program for Tennessee. U.S. Geol. Survey open-file report., Nashville, Tenn.
- Moore, G. K. 1988. Concepts of groundwater occurrence and flow near Oak Ridge National Laboratory, Tennessee. ORNL/TM-10969.
- NOAA (National Oceanic and Atmospheric Administration). 1974. Tennessee. pp. 370-384. In *Climates of the States*, vol. I--Eastern States. Water Information Center, Port Washington, N. Y.
- Peters, L. N., D. F. Grigal, J. W. Curlin, and W. J. Selvidge. 1970. Walker Branch Watershed project: chemical, physical, and morphological properties of the soils. ORNL/TM-2968.
- Sledz, J. J., and D. D. Huff. 1981. Computer model for determining fracture porosity and permeability in the Conasauga Group. ORNL/TM-7695.
- Solomon, D. K., G. K. Moore, L. E. Toran, R. B. Dreier, and W. M. McMaster. 1992. Status report. A hydrologic framework for the Oak Ridge Reservation. ORNL/TM-12,026.
- Solomon, D. K., and G. T. Yeh. 1987. Application of 3-D FEMWATER to the study of trench "bathtubbing." ORNL/RAP/LTR-87/89.
- Switek, J., C. S. Haase, and S. H. Stow. 1987. Geochemistry of formation waters in the lower Conasauga Group: Preliminary data from the Rock Cover (RCD) wells. ORNL/RAP-5
- TDWR (Tennessee Division of Water Resources). 1961. Tennessee's water resources. Tennessee Department of Conservation and Commerce, Nashville, Tenn.

- Toran, L. E., D'Azevedo, and O. M. Reyes. 1992. Modification of FEMWATER for parallel computing. American Geophysical Union Spring Meeting, Montreal, Canada, May 12-16, Proceedings.
- Toran, L. E., and J. A. Saunders. 1992. Geochemical and groundwater flow modeling of multiport-instrumented coreholes (GW-131 to GW-135). Y/TS-875.
- Toran, L. E., D. K. Solomon, W. M. McMaster, and C. M. Morrisey. 1991. Matrix diffusion as a mechanism to explain recent tritium and old 14-C in groundwater from fractured sedimentary rocks. American Geophysical Union Spring Meeting, Baltimore, May 28-31, Proceedings.
- Tucci, P., 1986. Ground-water flow in Melton Valley, Oak Ridge Reservation, Roane County, Tennessee--Preliminary model analysis. U.S. Geol. Survey Water Resources Investigation Report (WRIR) 85-4221, Nashville, Tenn.
- Webster, D. A. 1976. A review of hydrologic and geologic conditions related to radioactive solid-waste burial grounds at Oak Ridge National Laboratory, Tennessee. U.S. Geol. Survey open-file report 76-727, Nashville, Tennessee.
- Webster, D. A., and M. W. Bradley. 1987. Hydrology of the Melton Valley radioactive-waste burial grounds at Oak Ridge National Laboratory, Tennessee. U.S. Geol. Survey Open-File Report. 87-686, Nashville, Tennessee.
- Wickliff, D. S., D. K. Solomon, and N. D. Farow. 1991. Preliminary investigation of processes that affect source term identification. ORNL/ER-59.

# APPENDIX

PROCEDURES USED TO OBTAIN DATA THAT ARE DESCRIBED  
OR INTERPRETED IN THE TEXT



## A.1 PROCEDURES FOR INJECTION TESTS

Thirty-nine injection tests were made in Melton Valley (ORR aquitards) by pumping water from a plastic tank into a well with a peristaltic pump or a small submersible pump. The injection rate was adjusted with a speed controller on the pump and was measured at the end of the injection period with a stopwatch and a container. The injection rates for 39 tests had a range of 0.018-1.8 gallons per minute (gpm). Water levels were monitored with pressure transducers. The objective during the injection period was to maintain a nearly constant water level near the top of the casing or >10 ft above the static level to maximize the aquifer volume that was tested. The injection rate was adjusted as needed during the first 15 min of the test but was not changed during the last 30 min. Injection was continued until there was <0.1 ft of water level change in 5 min; the typical injection period was 1 h. After injection was stopped, water level recovery was monitored for a period of 4-24 h.

Analysis of the recovery data for an injection test began with a graph of water level versus log time for detection of any anomalies in the data. A graph of log water level versus log time was also made for a few tests; a straight-line trend shows that early data are affected by borehole water storage (Novakowski 1990, p. 100). The Theis recovery method (Theis 1935, p. 522) produced the best results for analysis of the data from most injection wells. Driscoll (1986, pp. 252-260) describes interpretations of Theis recovery graphs but omits effects of borehole water storage. A long delay (>10 min) in the beginning of a straight-line trend on the Theis recovery graph causes oversteepening of the line. Transmissivity is calculated from the slope of a water level recovery graph or the Theis recovery graph.

Storativity cannot be calculated from the injection test data, but from Darcy's law and the cubic law for groundwater flow in a fracture (Domenico and Schwartz 1990, p. 87),

$$Q = KIA = (gb^2/12v)I(bW) , \quad (1)$$

where  $Q$  is flow rate,  $K$  is hydraulic conductivity,  $I$  is hydraulic gradient,  $A$  is cross sectional area,  $g$  is acceleration of gravity,  $v$  is kinematic viscosity of water,  $b$  is aperture, and  $W$  is width of the fracture orthogonal to the groundwater flow direction. At 58°F,  $v = 0.100 \text{ m}^2/\text{d}$ , and  $g = 7.32 \times 10^{10} \text{ m}/\text{d}^2$ . For  $T$  in  $\text{m}^2/\text{d}$  and  $b$  in  $\text{m}$ ,

$$g/12v = 6.07 \times 10^{10} ,$$

$$Q = 6.07 \times 10^{10} (b^2) I(bW) , \quad (2)$$

$$T = Kb = 6.07 \times 10^{10} b^3 , \quad (3)$$

$$b = (1.65 \times 10^{-11} T)^{1/3} . \quad (4)$$

Equation (4) can be used to calculate fracture aperture from the transmissivity value measured with an injection test. If fracture spacing is known or can be estimated, a one-dimensional measure of fracture porosity (Snow 1968, p. 80) is

$$\theta = b/\Delta , \quad (5)$$

where  $\theta$  is fracture porosity, and  $\Delta$  is fracture spacing.

If an average permeable interval is assumed to represent a continuum, Darcy's law for a hydrologic section is

$$Q = KIW\Delta . \quad (6)$$

From Eq. (2) and (6), as was shown by Snow (1968, p. 79),

$$6.07 \times 10^{10} b^3 IW = KIW\Delta ,$$

$$K = 6.07 \times 10^{10} b^3 / \Delta = T / \Delta . \quad (7)$$

Equation (7) can be used to calculate the average hydraulic conductivity of a permeable interval. The transmissivity values of Eq. (3) and (7)) are the same, but the hydraulic conductivity is several orders of magnitude smaller in the continuum than in the fracture. Thus, transmissivity is the parameter that links fracture flow to the flow rate of a continuum.

## A.2 PROCEDURES FOR HYDROGRAPH ANALYSIS

Various equations, derived from heat-flow theory and conservation of mass, can be used to calculate groundwater discharge from an isotropic and homogeneous aquifer of limited areal extent. Examples include Glover (1964, pp. 36-48); Rorabaugh (1960, 1964); UNESCO (1975); and Walton (1970, pp. 174-188). However, these equations assume a constant transmissivity and do not produce reasonable results on the ORR where most subsurface water flows through the stormflow zone and the water table interval of the groundwater zone. These thin layers are drained or partly drained between recharge events, and transmissivity changes with time.

In areas of the ORR aquitards, hydrographs are representative of discharges from the stormflow and groundwater zones only during the nongrowing season, when evapotranspiration is slow and has minimal effects on flow processes. During this period, hydrographs of both streamflow rates and water levels in stormflow monitoring tubes peak within a few hours of peak rainfall intensity. The average delay for peak water levels in observation wells is 4 d (Moore 1989, p. 36).

During the following recessions of water levels, graphs of log water-level stage vs time plot as straight lines in both the stormflow and groundwater zones. A plot of log streamflow versus time forms a straight line after the end of overland runoff, and the average slope of this line is nearly the same as that of average stage recession in the stormflow zone. After a few more days of recession, the streamflow data curve and then plot as a straight line with an average slope that is nearly the same as that of the average water level recession in observation wells. The close correspondence of the semilog recession rates shows that nearly all streamflow at high-base flows is produced by discharge from the stormflow zone, whereas discharge from the groundwater

zone is dominant at lower base flows, after the stormflow zone has drained (Moore 1992).

During the growing season, hydrographs in areas of the ORR aquitards have different characteristics. Water levels in observation wells generally decline, and there are fewer and smaller recharge events because of larger soil water deficits. Also, consumption of water from the stormflow zone by evapotranspiration causes the stage hydrograph to curve after a few days of recession. Nearly all streamflow during the growing season consists of overland runoff from saturated soils because the streamflow recession slopes are steeper and occur sooner than do stage recessions in the stormflow zone.

There are not detailed records of water levels in observation wells and stormflow monitoring tubes in areas of the Knox aquifer; all interpretations are made from the hydrograph of Ish Creek. The steep streamflow recession slopes that are typical of overland runoff are uncommon in these areas. During both the nongrowing and growing seasons, most precipitation events result in an early streamflow recession that is typical of stormflow discharge and a later recession that is typical of groundwater discharge. The deeper water table in these areas apparently results in less water consumption by evapotranspiration.

The correspondence of the semilog recession rates of streamflows with water levels in stormflow monitoring tubes and, later, with water levels in observation wells can be expressed as

$$\ln(Y_1/Y_2)/(t_2 - t_1) = \lambda = \ln(Q_1/Q_2)/(t_2 - t_1) , \quad (1)$$

where  $Y_1$  is water-level stage and  $Q_1$  is streamflow rate at time  $t_1$ ,  $Y_2$  is stage and  $Q_2$  is streamflow at time  $t_2$ , and  $\lambda$  is the slope of the graph in units of inverse time. In order to avoid confusion,  $\lambda$  is shown as a positive value in this appendix.

The relationship of base streamflow to changes in the volume of subsurface water storage can be expressed, for example, as

$$V_1 = Q_1(t_2 - t_1)/\ln (Q_1/Q_2) , \quad (2)$$

and from Eq. (1),

$$V_1 = Q_1/\lambda , \quad (3)$$

$$V_t = Q_t/\lambda , \quad (4)$$

where  $V_1$  is volume of water storage at time  $t_1$ ,  $Q_1$  is the streamflow rate produced by the stored water,  $Q_2$  is the streamflow rate at a later time, and  $V_t$  and  $Q_t$  are the same parameters at time  $t$  during a recession. The change in storage volume is related to the change in streamflow by

$$(V_1 - V_2) = (Q_1 - Q_2)/\lambda . \quad (5)$$

The change in storage volume can also be expressed as

$$(V_1 - V_2) = AS_y(Y_1 - Y_2) , \quad (6)$$

and the volume of water in storage at any time,  $t$ , is

$$V_t = AS_yY_t , \quad (7)$$

where  $A$  is drainage area and  $S_y$  is specific yield. Combining Eq. (4) and (7),

$$Q_t/\lambda = AS_yY_t ,$$

$$S_y = Q_t/\lambda AY_t . \quad (8)$$

The average specific yield of a hydrologic unit can thus be determined from streamflow rate, water-level stage, and the semilog recession slope.

When the incremental recessions of streamflow and stage are exponential with time, water-level profiles can be assumed to have a stable shape, and Darcy's law should relate discharge to the hydrology of the stormflow zone and the groundwater zone. For discharge from both sides of a stream, the general equation is

$$Q_t = 2T_t I_t L_t , \quad (9)$$

where  $T_t$  is transmissivity,  $I_t$  is hydraulic gradient, and  $L_t$  is total length of gaining stream channels. The subscript indicates that the parameter is not constant, and that the value at time  $t$

should be used in the equation. Stream channels are convergent in a basin, but can be assumed to be evenly spaced because channel length has a linear relationship with discharge. For this case,

$$L_t = A_t/2a_t , \quad (10)$$

$$Q_t = T_t I_t A_t / a_t , \quad (11)$$

where  $a_t$  is path length, the average distance from a drainage divide to a stream.

During droughts, the stormflow zone is drained, and the water-table interval of the groundwater zone is partly drained. Decreases in saturated thickness produce corresponding decreases in transmissivity and length of flowing streams. Smaller changes occur in hydraulic gradients, which are partly determined by the slopes of the base of the stormflow zone and the base of the permeable layer near the water table. An assumption of a constant hydraulic gradient probably results in only a minor error in any calculation because contour maps of water-table elevation show only small seasonal changes in hydraulic gradient.

A logical approach to changes in the other parameter values [Eq. (11)] consists of estimating path length near the time of peak discharge, when the entire watershed is contributing to streamflow. Based on this assumption, Eq. (3) and (8) indicate

$$Q_o = \lambda V_o = \lambda A S_y Y_o , \quad (12)$$

where  $Q_o$ ,  $V_o$ , and  $Y_o$  are the values at the time of peak discharge. Combining equations (11) and (12),

$$\begin{aligned} T_o I / a_o &= \lambda S_y Y_o , \\ T_o &= a_o \lambda S_y Y_o / I . \end{aligned} \quad (13)$$

Equation (13) can be used to calculate the peak transmissivity of either the stormflow zone or the groundwater zone. Both values represent an average for the basin. The application of equations (8) and (13) for calculation of specific yield and transmissivity in the headwaters of Melton Branch (ORR aquitards) is shown in Moore (1992, pp. 393-394).

### A.3 PROCEDURES FOR BOREHOLE FLOWMETER SURVEYS

The borehole flowmeter, which was recently invented by the Engineering Laboratory of Tennessee Valley Authority, consists of a metal cylinder about 8 in. long and about 2 in. in diameter with a center hole for water flow; the hole is 0.5 or 1.0 in. in diameter and is flared at the top and bottom to reduce turbulence. Two chloride electrodes contact the water in the center hole, and a magnetic coil is contained in the body of the cylinder. A multiconductor electrical cable is used to supply power to the coil and to carry the signal to the surface for processing. A flow of water through the center hole acts as a conductor, and the interaction of the conductor and the coil is measured as a voltage. The water must have some dissolved solids, but the constituents and concentrations of these solutes do not affect the measurements. The flowmeter fits tightly in a 2-in. inside diameter well casing, but for larger diameter wells, a packer is used to fill the annulus between the instrument and the wall of the well. The packer ensures that all vertical flows pass through the center hole in the flowmeter.

The borehole flowmeter produces an absolute measurement of the flow rate up or down a well at a selected depth position; the relative change in flow rate between two depth positions indicates whether or not a pervious fracture occurs in the interval. If a well has no natural flow, flows are induced by pumping or injecting water. Measurements of flow are more reliable if water velocity is much larger than the minimum detectable signal. For this reason, it is desirable to select a water injection rate that is as large as possible.

The first task at a well that has no natural flow is to begin water injection at a constant rate. In response, the water level in the well rises, rapidly at first and then progressively more

slowly with time. A nearly constant water level, which generally occurs after 15-30 min of injection, is indicative of a nearly steady water velocity at any depth in the well. These are the conditions needed for a reliable flowmeter survey. To maintain the nearly constant water level and water velocity, the injection rate can be changed slightly during the flowmeter survey.

Perturbations in water velocity and instrument signal are produced by moving the flowmeter up or down the well. After positioning the instrument at a selected depth, it is necessary to wait 1-3 min for the instrument readings to stabilize. The voltage signal is then sampled repetitively; the samples are averaged over a selected period of time, and the depth and flow rate are recorded in digital form and on paper. Some signals have little fluctuation and need to be averaged over only a 15- to 30-s interval. Noisy signals can be averaged for 30-60 s or longer. The variance of the signal can be recorded as can the flow rate in both gallons per minute (gpm) and volts.

There are various sources for error in flow measurements, and the precision of the flowmeter data is difficult to determine numerically. The two main problems are noisy data, probably caused by water turbulence or external electrical currents, and a bypass of water around the instrument. Water bypass can be caused by poor packer seals and by permeable pathways in fractures and sandpacks adjacent to the borehole. However, the flowmeter data show that many sequential flow rates differ by  $<0.005$  gpm and that wells with sandpacks show abrupt changes in flow rate at the top and bottom of permeable fractures rather than the gradual changes that would be expected for water bypass. The surveys also show nearly the same change of flow rate with depth (a nearly constant first derivative) within the permeable intervals of the wells. These data characteristics indicate a good precision and a satisfactory accuracy for the flowmeter surveys.

The borehole flowmeter data on the ORR have been used to select monitoring depths in newly constructed wells, to check the accuracy of screen depths in well-construction archives, to evaluate the potential for cross contamination (a flow of pollutants in a well from one level to another), and to characterize permeable fractures in the rock (Moore and Young 1992).

#### A.4 REFERENCES

- Domenico, P. A., and F. W. Schwartz. 1990. Physical and Chemical Hydrogeology. Wiley, N. Y.
- Driscoll, F. G. 1986. Groundwater and Wells. Johnson Division, St. Paul, Minn.
- Glover, R. E. 1964. Ground-water movement. U.S. Bur. of Reclam. Eng. Mono. no. 31.
- Moore, G. K. 1989. Groundwater parameters and flow systems near Oak Ridge National Laboratory, Tennessee. ORNL/TM-11368.
- Moore, G. K. 1992. Hydrograph analysis in a fractured rock terrane. Ground Water 30(3):390-395.
- Moore, G. K., and S. C. Young. 1992. Identification of groundwater producing fractures by using an electromagnetic borehole flowmeter in monitoring wells on the Oak Ridge Reservation, Oak Ridge, Tennessee. ORNL/ER-91.
- Novakowski, K. S. 1990. Analysis of aquifer tests conducted in fractured rock: a review of the physical background and the design of a computer program for generating type curves. Ground Water, 28(1):99-107.
- Rorabaugh, M. I. 1960. Use of water levels in estimating aquifer constants. pp. 314-323. In Intern. Assoc. of Scientific Hydrology, General Assembly of Helsinki, Pub. No. 52, Proceedings.
- Rorabough, M. I. 1964. Estimating changes in bank storage and ground-water contribution to streamflow. pp. 432-441. IN Intern. Assoc. Scientific Hydrology, Symposium [on] Surface Waters, Pub. No 63, Proceedings.
- Snow, D. T. 1968. Rock fracture spacings, openings, and porosities. J. Soil Mech. Found. Div., Proc. Am. Soc. Civil Engrs. 94:73-91.

- Theis, C. V. 1935. The relation between the lowering of the piezometric surface and the rate and duration of discharge of a well using ground-water storage. pp. 519-524. In: Am. Geophys. Union Ann. Meeting, 16th, transactions, pt. 2, Section of Hydrology. National Research Council, Wash., D.C.
- UNESCO. 1975. Chapt. 5. Defining the water balance. In Ground-Water Studies, an International Guide for Research and Practice. UNESCO Press, Paris, France.
- Walton, W. C. 1970. Groundwater Resource Evaluation. McGraw-Hill, N. Y.

1  
2  
3

4  
5  
6

7  
8  
9

## Internal Distribution

1. T. L. Ashwood
2. L. D. Bates
3. F. P. Baxter
4. D. M. Borders
5. H. L. Boston
6. J. W. Bownds
7. H. M. Braunstein
8. J. B. Cannon
9. R. B. Clapp
10. K. W. Cook
11. T. K. Cothron
12. N. H. Cutshall
13. J. H. Cushman
14. M. F. P. DeLozier
- 15-19. R. B. Dreier
20. T. O. Early
21. T. A. Fontaine
22. J. M. Forstrom
23. C. W. Francis
24. D. W. Frazier
25. B. J. Frederick
26. D. E. Fowler
27. S. B. Garland, II
28. C. W. Gehrs
29. P. L. Goddard
30. B. K. Harrington
31. R. D. Hatcher
32. D. S. Hicks
33. S. G. Hildebrand
34. Lucius Holder, Jr.
- 35-54. D. D. Huff
55. G. K. Jacobs
56. S. B. Jones
57. P. M. Jardine
58. P. Kanciruk
59. R. H. Ketelle
60. B. L. Kimmel
61. A. J. Kuhaida
62. R. R. Lee
63. S. Y. Lee
64. P. J. Lemiszke
65. R. S. Loffman
66. R. J. Luxmoore
67. L. W. McMahon
68. C. M. Morrissey
- 69-88. G. K. Moore
89. P. J. Mulholland
90. J. B. Murphy
91. C. E. Nix
92. M. J. Norris
93. J. E. Nyquist
94. F. S. Patton, Jr.
95. T. Purucker
96. D. E. Reichle
97. C. T. Rightmire
98. M. W. Rosenthal
99. T. H. Row
100. P. A. Rubin
101. W. E. Sanford
102. F. E. Sharples
- 103-106. L. A. Shevenell
107. L. G. Shipe
108. R. L. Siegrist
109. D. S. Shriner
110. E. D. Smith
- 111-125. D. K. Solomon
126. B. P. Spalding
127. S. H. Stow
128. D. W. Swindle
129. M. F. Tardiff
- 130-149. L. E. Toran
150. J. R. Trabalka
151. J. E. Van Cleve
152. R. I. Van Hook
153. J. C. Wang
154. D. R. Watkins
155. O. R. West
156. R. K. White
157. S. L. Winters
158. T. F. Zondlo
- 159-167. ESD Library
168. Central Research Library
169. ORNL Y-12 Technical Library
- 170-171. Laboratory Records Department
172. Laboratory Records, ORNL-RC
173. ORNL Patent Office

## External Distribution

174. Jerry Archer, Geraghty and Miller Inc., 97 Midway Lane, Oak Ridge TN 37830
175. Richard Arnseth, SAIC, 301 Laboratory Road, Oak Ridge TN 37830
176. Ernest Beauchamp, C-260 Jackson Plaza, MS: 7614, Rm 13, Oak Ridge TN 37830
177. Robert Benfield, TDEC/DOE Oversight, 761 Emory Valey Road, Oak Ridge TN 37830
178. G. W. Bodenstein, USDOE-OR Federal Bldg, Oak Ridge TN 37830
179. Paul Craig, Environmental Consulting Engineers (ECE), P.O. Box 22668, Knoxville RTN 37933
180. S. N. Davis, 6540 Box Canyon DSrive, Tucson AZ 85745
181. Director, Center for Management, Utilization, and Protection of Water Resources, Tennessee Technological University, P.O. Box 5082, Cookeville TN 38505
182. R. N. Farvolden, Waterloo Centre for Groundwater Research, University of Waterloo, Waterloo, Ontario N2L-361 Canada
183. J. F. Franklin, Bloedel Professor of Ecosystem Analysis, College of Forest Resourcesa, Anderson Hall AR-10, Un9iversity of Washington, Seattle WA 98185
184. C. S. Haase, 603 School of Mines Road, Socorro NM 87801
185. Jim Harless, TDEC/DOE Oversight, 761 Emory Valley Road, Oak Ridge TN 37830
186. R. C. Harriss, Institute for the Study of Earth, Oceans, and Space, Science and Engineering research Bldg, University of New Hampshire, Durham NH 03824
187. G. M. Hornberger, Professor, Department of Environmental Sciences, University of Virginia, Charlottesville VA 22903
188. G. Y. Jordy, Director, Office of Program Analysis, office of Energy research, ER-30, G-226, USDOE, Washington, D.C. 20545
189. P. E. Lamoreaux and Associates Inc., P.O. Box 2310, Tuscaloosa AL 35403
190. W. M. McMaster, 1400 West Racoon Valley Road,
191. Manager, Bechtel National Inc, 151 Lafayette Drive, Oak Ridge TN 37830
192. Manager, CH2M Hill, 599 Oak Ridge Turnpike, Oak Ridge TN 37830

193. Manager, HSW Environmental Consultants 687 Emory Valley Road, Oak Ridge TN 37830
194. Manager, Radian/Lee Wan Associates, 120 South Jefferson Circle, Oak Ridge TN 37830
195. Manager, Systematic Management Services, 673 Emory Valley Road, Oak Ridge TN 37830
196. Ronit Nativ, Dept. of Soil and Water Sci., Faculty of Agriculture, Hebrew University of Jerusalem, P.O. Box 12, Rehovot 76100 Israel
197. Chudi Nwangwa, TDEC/DOE Oversight, 761 Emoe Valley road, Oak Ridge TN 37830
198. R. H. Olsen, Professor, Microbiology and Immunology Dept., University of Michigan, Medical Sciences II, #5605, 1301 East Catherine Street, Ann Arbor MI 48109-0620
199. A. Patrinos, Acting Director, Environmental Sciences Division, Office of Health and Environmental Research, ER-74, USDOE, Washington D.C. 20585
200. William K. Puff, Dames and Moore, 575 Oak Ridge Turnpike, Oak Ridge TN 37830
201. James F. Quinlan, Quinlan and Associates, P.O. Box 110539, Nashviulle TN 37222
- 202-206. Fred Quinones, Chief, Tennessee District, WRD, U.S. Geological Survey, 810 Broadway, Suite 500, Nashville TN 37203
- 207-208. Gregory D. Reed, Chairman, Dept. of Civil Engineering, University of Tennessee, 62 Perkins Hall, Knoxville TN 37996-2010
209. Debra Shults, Tennessee Dept. of Environment and Conservation, Div. of Radiological Health, TERRA Bldg., 150 Ninth Ave., North, Nashville TN 37243-1532
210. William C. Sidle, Environmental Protection Division, USDOE-OR, P.O. Box 2001, Oak Ridge TN 37831-8739
211. James Smoot, Department of Civil Engineering, University of Tennessee, 62 Perkins Hall, Knoxville TN 37996-2010
212. F. J. Wobber, Environ. Sciences Div., Office of Health and Environmental Research , Office of Energy Research, ER-74, USDOE, Washington, D.C. 20585
213. John Young, Camp Dresser & McGee, Suite 500, 800 Oak Ridge Turnpike, Oak Ridge TN 37830
214. Steven C. Young, TVA Engineering Laboratory, P.O. Box E, Norris TN 37828

215. Office of Assistant Manager for Energy Research and Development, USDOE-OR,  
P.O. Box 2001, Oak Ridge TN 37831-8600

216-225. Office of Scientific and Technical Information, P.O. Box 62, Oak Ridge  
TN 37831